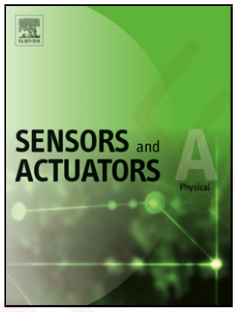

Title: Room-temperature gas sensing of ZnO-based gas sensor: A review

Authors: Ling Zhu, Wen Zeng

PII: S0924-4247(17)31465-6
DOI: https://doi.org/10.1016/j.sna.2017.10.021
Reference: SNA 10387

To appear in: *Sensors and Actuators A*

Received date: 12-8-2017
Revised date: 29-9-2017
Accepted date: 7-10-2017

Please cite this article as: Ling Zhu, Wen Zeng, Room-temperature gas sensing of ZnO-based gas sensor: A review, Sensors and Actuators: A Physical https://doi.org/10.1016/j.sna.2017.10.021

Room-temperature gas sensing of ZnO-based gas sensor: A review

Ling Zhu, Wen Zeng[1*]

College of Materials Science and Engineering, Chongqing University, Chongqing China

Abstract

Novel gas sensors with high sensing properties, simultaneously operating at room temperature are considerably more attractive owing to their low power consumption, high security and long-term stability. Till date, zinc oxide (ZnO) as semiconducting metal oxide is considered as the promising resistive-type gas sensing material, but elevated operating temperature becomes the bottleneck of its extensive applications in the field of real-time gas monitoring, especially in flammable and explosive gas atmosphere. In this respect, worldwide efforts have been devoted to reducing the operating temperature by means of multiple methods. In this communication, room-temperature gas sensing properties of ZnO based gas sensors are comprehensively reviewed. Much more attention is particularly paid to the effective strategies that create room-temperature gas sensing of ZnO based gas sensors, mainly including surface modification, additive doping and light activation. Finally, some perspectives for future investigation on room-temperature gas-sensing materials are discussed as well.

Keywords: ZnO; semiconductor material; gas sensing; room-temperature operation

* Corresponding author E-mail: wenzeng@cqu.edu.cn (W. Zeng)

1. Introduction

Over the last few decades, with the rapid development of industrialization and urbanization, the severe air pollution primarily attributed to automobile exhaust and factory emission has become a great threat to human survival and development. Meanwhile, a leakage of flammable and explosive gases may result in loss of life and property damage. So, real-time and effective detection of those harmful gases via using gas sensors is in pressing need at present. Off all the numerous semiconductor gas sensors, semiconducting metal oxide based gas sensors have received wide research around the globe by virtue of their high gas response, excellent selectivity, good portability, and low fabrication cost [1-6].

ZnO, as typical n-type semiconductor, exhibits unique characterizations required for an ideal gas sensor such as wide band gap of 3.37 eV, large exciton binding energy of 60 meV, high electron mobility, photoelectric response, excellent chemical and thermal stability [7-12]. Meanwhile, ZnO has the merits with low-cost, non-toxic, easy preparation and suitable for high mass production [13]. Moreover, ZnO is a typical chemoresistive sensing material. Its gas sensing is dominantly controlled by the change in sensor resistance when gas molecules react to its surface [14]. In ambient atmosphere, oxygen molecules are adsorbed on the surface of ZnO and then ionize into oxygen species by capturing electrons from the conduction band, leading to the formation of surface depletion layer and thus increasing the sensor resistance. When reductive gas such as acetone, approach ZnO surface, the oxygen species will interplay with these gas molecules and release trapped electrons back to the conduction band,

causing the sensor resistance to decrease [15, 16]. While exposure to oxidative gases such as NO_2 acted as electron acceptor, the sensor resistance increases instead [17, 18]. Hence, it is the variation of sensor resistance that achieves the gas sensing detection.

As well known, gas sensing performances of ZnO based gas sensors are largely dependent on its operating temperature that controls the reaction kinetics, conductivity and electron mobility [19-21]. Generally, traditional ZnO gas sensors are run by an elevated temperature of 300-500ºC [21-25], since enough thermal energy of surface redox reaction is required to overcome the activation energy barrier and increase the reaction kinetics in order to realize sensing measurement [26-28]. Whereas high-temperature operation adversely limits its wide application, because high temperature signifies energy waste that runs in the opposite direction in our society advocating energy conservation and emission reduction. Furthermore, gas explosion is most likely to occur as flammable and explosive gases have low ignition point in normal atmosphere [29]. In addition, high-temperature operation also causes the sensor instability which may lead to imprecise or incorrect test results [30, 31]. The urgent task, therefore, is to reduce the operating temperature of ZnO based gas sensors.

ZnO based gas sensors operating at room temperature that do not require heating devices are more portable and cost effective, according with the current developing trend. Most importantly, room-temperature operation makes it possible to reduce energy use and risk of gas explosion as well as improve the long-term stability, and this has become an evolving topic. In contrast, thermally induced growth of ZnO grains is easily generated owing to high operating temperature, then affecting gas diffusion at

the grain boundaries, which is responsible for the undesirable long-term drift problem caused by sintering effect [23, 32-35]. As a result, the sensor stability is reduced, followed by shortening of service life. Fortunately, room-temperature operation of ZnO based gas sensors exactly avoids or reduces the above problem and makes a great improvement in long-term stability.

However, the small amount of thermal electrons could be found on ZnO surface when the sensor is operated at room temperature, forming few oxygen species because of low thermal energy. These very limited number of oxygen species is thermally stable and difficult to remove from the surface due to large adsorption energy, resulting in low sensing properties [13, 32, 36, 37]. Beyond these, relative humidity (RH) is one of the predominant disturbing factors of room-temperature operation of ZnO based gas sensors [38, 39]. In wet atmosphere, H_2O molecules will compete for the surface reaction sites with oxygen molecules and in-turn limit oxygen adsorption. The number of oxygen species will decrease with the increase of RH level, causing a decline of baseline resistance in ambient atmosphere with lower sensor response [29, 40-42]. The charge carrier transport might be attributed to chemisorbed mechanism at lower RH and Grotthuss mechanism by physisorption at higher RH level, respectively, as shown in **Fig. 1** [39, 43, 44]. Therefore, influence of RH should be taken into consideration while investigating room-temperature gas sensing properties. In previous studies, the room-temperature gas sensing properties have been measured in dry air or at several different constant RH levels. In brief, the biggest challenge we face at present is to reduce the operating temperature of ZnO sensors.

Although there are already a host of reports that have made certain progress on reducing the operating temperature of ZnO based gas sensors to some degree, the temperature is still a little high, not at room temperature. Madhumita Sinha et al. [45] synthesized ZnO nanowires by hydrothermal method as the sensing layer. The fabricated sensors exhibited ultrahigh response of 98% to 100 ppm H_2 at 250^{o}C. T. Tesfamichael et al. [46] prepared W-doped ZnO thin film using magnetron sputtering. It was observed that the hybrid sensor showed significant higher sensing performance towards 5-10 ppm NO_2 at low operating temperature of 150^{o}C. R Dhahri et al. [47] reported that Ag-modified In_2O_3/ZnO nanobundles with porous structure prepared by a hydrothermal method continuing with dehydration process. The as-prepared sensor showed response time of 12 s and recovery times of 6 s to the detection limit of 100 ppb formaldehyde (HCHO) at lower temperature of 100^{o}C. A brief summary of some examples about current development of ZnO based gas sensors working at relatively high temperature is listed in **Table 1**. However, that's far from enough. Much effort has been made to further reduce the operating temperature to room temperature. Some effective strategies primarily including surface modification based pure ZnO nanostructure, additive doping and exposure of ZnO based gas sensors to ultraviolet (UV) or visible light illumination have been widely utilized, and enhanced mechanisms of these three techniques are different. Detailed explanation can be found in following section 2-4.

To the best of our knowledge, in recent years, a lot research on ZnO based gas sensors operating at room temperature has witnessed significant progress, yet a review

on this subject is still missing up to now. In this review, we intend to comprehensively summarize the room-temperature gas sensing properties of ZnO based gas sensors. While Zhang and coworkers [48] have reported the nanostructured materials for room-temperature gas sensors, which focus on different nanostructured materials including single-element materials, metal-oxide-based nanostructures, organic semiconductors and carbon nanostructures and highlight the structure-property correlation, here we would like to specifically discuss the effective strategies and mechanisms that create room-temperature gas sensing performance of ZnO based gas sensors, and hope to provide an insight for future investigation on room-temperature gas sensing materials.

It must be said, though, that ZnO loaded carbon composite materials where ZnO acts as the second component is also effective to reduce the operating temperature [27, 49-51], but it is not our focus this time and will not be discussed here.

2. Surface modification

Due to small size with large surface to volume ratio and more surface active sites to the environment, nanostructured ZnO has a significant portion of surface atoms than bulk atoms, demonstrating a potential for use as the sensing layer. It is found that grain size of nanostructured ZnO has a major influence on its sensor response [36, 62]. When the grain size is close or smaller than twice Debye length (depth of the space-charge layer), the response greatly relies on it and can be exponentially increased with the decrease of the grain size. While the grain size is far larger than twice Debye length, the gas sensing is controlled by the contact potential barrier rather than the grain size [63-65]. Many studies have concentrated on the decrease in grain size of nanostructured

ZnO to enhance the room-temperature gas sensing. However, the grain size is inversely proportional to the van der Waals force promoting particle agglomeration. Thereby the grain size could not be blindly reduced. In that case, it not only decreases the specific surface area, but also restricts the gas diffusion between particles [66]. Besides, a much smaller grain size of ZnO is often accompanied by a drop of thermal stability [67]. Apart from the grain size, the effect of surface morphologies, defects and porosity of ZnO nanostructures on gas sensing is of great importance. Different morphologies of ZnO nanostructures have different spatial structures and specific areas, leading to different abilities to gas diffusion during adsorption-desorption of gas molecules [68]. In addition, defects of nanostructured ZnO such as oxygen vacancies as electron donor are beneficial for the increase in conductivity of ZnO, facilitating the gas sensing properties and then reducing the operating temperature [18, 69, 70]. Beyond that, the effective gas diffusion channel is also increased with assistance of density of porosity [18]. Efforts of researchers have demonstrated that high surface to volume ratio, density of defects and porosity of ZnO nanostructures can contribute to the room-temperature gas sensing [48].

In general, surface morphological modification is performed by tuning the key parameters of various methods [43]. Synthesis parameters are optimized to control the nucleation and growth process of ZnO nanostructures in an effort to generate unique morphological sensing materials with high sensing properties [24, 43]. In particular, one-dimension ZnO nanostructures, such as nanotubes, nanorods, nanowires, nanofibers and some hierarchical architectures assembled by one-dimension

nanostructures, possess excellent conductivity. Their enhanced electron mobility promotes the effective separation of electrons and holes, which deceases the resistance. A large number of adsorbed oxygen species are easily created by the chemical reaction between the surface and adsorbed oxygen molecules. Thus the surface sensing reaction is accelerated, reducing the operating temperature and finally achieve room-temperature gas sensing [4, 45, 71-73].

Up to now, diverse morphological ZnO nanostructures have been brilliantly designed by worldwide researchers through various approaches to achieve room-temperature gas sensing of ZnO gas sensors. For example, Z.S. Hosseini et al. [29] reported that rather vertically aligned ZnO nanorods with flower-like structures (**Fig. 2**) showed the highest response of 581 towards 5 ppm H_2S at room temperature (**Fig. 3**a) and a good selectivity to H_2S especially at room temperature (**Fig. 3**b). Simple vapor phase transport method was employed to obtain the nanorods with diameter in the range of 300-400 nm and length in the range of 7-9.5 μm. The nanorods formed a porous network consisting of directional channels for gas diffusion in and out. Because of the flower-like structure, the effective surface area was increased and lead to enhancement of gas sensitivity. Furthermore, the response in different relative humidity was measured (**Fig. 3**c), and good sensing behavior was observed even after more than 5 months of storage in air (**Fig. 3**d).

Lingmin Yu and co-workers [18] demonstrated that two-dimension(2-D) ZnO nanowalls (**Fig. 4**) were fabricated by facial solution method under various annealing temperature ranging from 350°C to 750°C. The nanowalls annealing at 450°C exhibited

excellent NO_2 gas response magnitude and fast response (23 s) and recovery time (11 s) at room temperature (**Fig. 5**a and b). The observed gas response magnitude showed no linear change with the increase of annealing temperature that represented the oxygen vacancy defects as shown in **Fig. 5**c. The deterioration in the gas sensing properties above the annealing temperature of 450^{o}C may be related to the decreased porosity, which was consistent with the SEM image shown in **Fig. 4**. Therefore, a delicate balance between vacancy defects and porosity dependent on the annealing temperature was the key factor for their good sensing properties. And the sensor also displayed good repeatability (**Fig. 5**d).

Jiabao Cui et al. [72] reported room temperature formaldehyde (HCHO) gas sensing of ZnO nanofibers, nanoplates, nanoflowers (**Fig. 6**a-f) successfully synthesized by simple electrospinning and hydrothermal routes, respectively. The ZnO nanofibers manifested a highest response **(Fig. 6**g) and fastest current response (32 s) and recovery time (17 s) at room temperature among the three morphologies. The authors ascribed the outstanding room-temperature gas sensing properties of ZnO nanofibers to the largest specific surface area (9.61 m^2/g) (**Table 2**). The nanofibers were composed of the minimum nanoparticles with an average size of 45 nm, thus they had a largest specific area. And there was a great number of grain boundaries for the nanofibers, causing a relatively thick depletion layer. Based on the adsorption gas sensing mechanism, the reaction between HCHO and oxygen species would take place when the nanofibers was exposed to the target gas, reducing the barrier height of grain boundaries. As a consequence, more electrons would pass through the grain boundaries,

resulting in the higher room-temperature sensor response for the ZnO nanofibers (**Fig. 6**h and i).

In this section, we summarize a part reports of room-temperature gas sensing properties of pure ZnO with different morphologies, as shown in **Table 3**. Overall, however, diverse ZnO nanostructures presents a relative low room-temperature gas sensing properties, so it is difficult to remarkably improve sensing properties of ZnO via simple surface modification. In other words, such method can only reduce the operating temperature to some degree. Better strategies are needed to further improve the room-temperature gas sensing properties of ZnO based gas sensors.

3. Additive doping

It is very appealing that room-temperature gas sensing of ZnO based gas sensors can also be realized through adding dopants as the secondary components into pure ZnO nanostructures, mainly containing metals, conducting polymers and inorganics. In this section, we will separately summarize the mechanism of each case. **Table 4** displays a part reports about room-temperature gas sensing properties of dopant/ZnO.

3.1. Metal adding

Different kinds of metal dopants such as noble metals (such as Au [93-95], Ag [96] and Pt [97]) and transition metals (such as Cu [76], Ni [78] and Co [98]) are always purposely selected for sensitization of ZnO sensing materials. Upon careful summarization we find that this sort of nanocomposites improves the reductive gas sensing behaviors at room temperature markedly.

More specifically, effect of noble metals on the enhancement of gas sensing properties of ZnO based gas sensors can be split into two categories: chemical effect and electric effect, depending on whether the noble metals modify the work function of ZnO [48, 99, 100].

Firstly, the chemical effect can be elucidated by spill-over phenomenon [95, 99]. Noble metals on ZnO surface promote adsorption and dissociation of atmospheric oxygen molecules into atomic species, which then migrate to ZnO surface and ionize into oxygen species by capturing electrons from the conduction band of ZnO. Therefore, the sensitization of noble metals increases the quantity of oxygen species and accelerates the surface reaction, causing an enlargement of the depletion layer followed by a higher baseline resistance (**Fig. 7**a and b). After exposed to reductive target gas, dissociation of target gas molecules also may occur owing to the catalysis of noble metals. The trapped electrons are easily released and injected into the conduction band, resulting in a remarkable decrease in depletion layer with a lower resistance. Then higher room-temperature gas sensing properties of ZnO based gas sensors are achieved in this way. For example, K. Shingange et al. [93] reported unloaded and loaded ZnO nanorods based sensors with different Au loading levels prepared by microwave-assisted method. It was observed that 0.5 wt% Au loaded ZnO sensor showed the highest sensing property and selectivity to NH_3 at room temperature explained by spill-over mechanism (**Fig. 8**a and b). In another instance, Duy-Thach and co-workers [97] compared the response behavior of ZnO dense films, ZnO nanoparticles and ZnO nanorods assisted by Pt towards H_2. The results demonstrated that sensing performance

of the chemiresistor sensor was improved due to the Pt catalyst, which was more efficient in dissociating H_2 gas molecules even at room temperature.

Secondly, the electric effect arises from the contact resistance of noble metal modified ZnO gas sensors [95, 101]. Electrons from conduction band of ZnO transfer into noble metals due to the difference in work function, forming the nano-Schottky barriers at the interface between noble metals and ZnO. As a result, additional depletion region near ZnO surface (**Fig. 7**c) is generated, reducing the room-temperature gas sensing performances.

In particular, sometimes joint action of chemical and electric effect promotes the development of room-temperature gas sensing performances of ZnO based gas sensors. For instance, Z.S. Hosseini et al [101] reported room-temperature H_2S gas sensing of Au sensitized vertical ZnO nanorods with flower-like structures via vapor phase transport method followed by sputtering. Different thicknesses of Au layer between 3 and 15 nm on ZnO surface achieved by setting the sputtering time in the range of 60-300 s (**Fig. 9**). The as-prepared sensor depicted variable response to different nominal Au layer thickness for 0.5 and 3 ppm H_2S at room temperature. The highest response was obtained for the Au (6 nm): ZnO sample **(Fig. 10**a). The response of the Au sensitized sensor was an approximately 3.7 times than the pure ZnO (**Fig. 10**b). The fabricated hybrid sensors also had higher selectivity to H_2S than the pure one at room temperature (**Fig. 10**c). And the Au (6 nm): ZnO sensor showed 2.5% variation in response with almost reproducible behavior (**Fig. 10**d). In their view, the enhanced room-temperature sensor response was ascribed to the spill-over effect, the formation

of Schottky barriers at Au–ZnO interface, more introduced surface active sites and effective surface area through surface coarsening (**Fig. 10**e).

Transition metal doping, always incorporating in ZnO thin film, can facilitate the room-temperature gas sensing properties as well. The enhanced mechanism can be interpreted using one or several following aspects: (1) ZnO grain size is changed when ZnO is modified by transition metals. It is well known that specific surface area of smaller grains can improve the gas sensing performances [102, 103]. (2) Complete morphological transformation and porosity are observed while transition metals are doped [98, 102, 103]. (3) More zinc vacancies are created, leading to an increase in charge carrier concentration [98]. (4) Zinc ions in ZnO lattice can be substituted by the transition metallic ions with similar radius to zinc ions and produce donor defects, promoting charge separation and transport [14, 103]. (5) p-n junction is formed between p-type dopants (Co, Ni and Cu) and n-type ZnO [98]. The enhancement of gas sensing because of p-n junction will be discussed in detail in the following section. All above can ultimately improve room-temperature gas sensing of ZnO based gas sensors. For example, Ganesh Kumar Mani and co-workers [98] synthesized undoped and transition metals (Co, Ni and Cu) doped ZnO nanoarchitectures via simple chemical spray pyrolysis technique (**Fig. 11**). The sensing response towards 10 ppm acetaldehyde was found to be 2.85, 800, 2.59 and 21.36 for the undoped, Co, Ni and Cu-doped ZnO nanostructures, respectively (**Fig. 12**a). The Co-doped ZnO nanostructure showed high selectivity towards acetaldehyde when exposed to 7 different vapors (**Fig. 12**b). **Fig.12**c and d manifested the response and recovery times toward acetaldehyde. High stability

nature of Co-doped ZnO thin film was also studied as shown in **Fig. 12**e. The structure and morphological results suggested that transition metals effectively altered the microstructures of ZnO. The formation of p-n junction and more zinc vacancies contributed to the ultrahigh response of Co-doped ZnO nanostructure at room temperature in addition to the changed morphology.

To sum up, different size, distribution, concentration and kinds of metal dopants all will affect room-temperature gas sensing properties of ZnO based gas sensors. So far most of studies are focused on the mono-metal doping, however, there are few reports about multi-metallic doping to achieve room-temperature gas sensing of ZnO sensors. Faying Fan et al. [104] did a research with regard to adding Pt-Au bimetallic nanoparticles into ZnO nanorods. The hydrogen sensing testing results at 130^{o}C indicated that the alloying nanoparticles loaded on ZnO showed larger response values than the mono-metallic nanoparticles loaded ZnO. In their report, the superior hydrogen sensing properties of (Pt-Au)-loaded ZnO was most probably ascribed to the strong hydrogen adsorption onto the Pt-Au bimetallic nanoparticles caused by the geometric and electronic effects between the two metals. The detailed mechanism has yet to be fully defined. According to this route, much can be done to further reduce the operating temperature of ZnO based gas sensors by multi-metallic doping.

3.2. Conducting polymer adding

Conducting polymers, such as Polypyrrole (PPy) [21], Poly(3-hexylthiophene) (P3HT) [70], polyaniline (PANI) [105], poly[N-9’-heptadecanyl-2,7-carbazole-alt-5,5-

(4',7'-di-2-thienyl-2',1',3'-benzothiadiazole)] (PCDTBT) [106], and poly (3,4-ethylenedioxythiophene) (PEDOT) [107-109] as the sensing materials have the superiority of high sensitivities, short response time and facile fabrication, especially they allow room-temperature operation. The advantages of using conducting polymers for gas sensors also have been thoroughly reviewed [110, 111].

With an aim to combine the merits of ZnO and conducting polymers, many efforts have been devoted to incorporating conducting polymers into ZnO to form hybrid nanocomposite sensing materials, hence creating room-temperature gas sensing. Such sensing enhancement mechanism can be explained by the formation of heterojunction with a hole-electron depletion layer at the interface of conducting polymers and ZnO. As a result of the concentration gradient of charge carriers, free electrons of n-type ZnO migrate toward the p-type conducting polymers with holes as the majority carriers. Meantime, the holes of conducting polymers will diffuse to ZnO. The energy bands bend and Fermi level finally attains a new balance, resulting in the formation of heterojunction at the interface. It is well known that the tunneling current across the heterojunction barrier has exponent relation to the junction barrier height [70]. In other words, the conductivity is extremely sensitive to small change in junction barrier height which relies on the depletion layer width [70, 112]. Once the sensors expose to target gas molecules, the width of depletion layer would be tuned, leading to a modulation in potential barrier height. Then, the current shows a fast change which is a strong symbol of higher gas sensing of ZnO based gas sensors.

Jing Wang et al. [70] reported a P3HT/ZnO hybrid sensing materials by a facile one-step solution method. The hybrid sensors (Fig. 13e) were fabricated for the detection of NO_2 at room temperature. In the process of preparing the hierarchical ZnO nanosheet-nanorod (NS-NR) architectures, the morphologies were different according to the aging time (**Fig. 13**a-c). It was observed that the P3HT/ZnO NS-NR bilayer film exhibited not only the highest sensitivity but also good reproducibility and selectivity to NO_2 at room temperature (**Fig. 13**e and f). They attributed the enhanced room-temperature sensing performances to the high content of oxygen-vacancy defects on the surface of NS-NR architectures, as well as the formation of the heterojunction formed at the interface between ZnO and P3HT (**Fig. 12**g).

As another example, Rakesh K. Sonker and co-workers [105] fabricated a ZnO-PANI hybrid composite sensor toward NO_2 operating at room temperature. They investigated the effect of concentration of PANI on NO_2 gas sensing. ZnO-PANI(5%) hybrid composite sensor showed the highest NO_2 gas sensing including response, response time and recovery time as shown in **Fig. 14**a-d. ZnO-PANI(5%) gave a maximum sensing response of ~6.11×10^2 towards 20ppm NO_2 with fast response and recovery time of about 2.16min and 3.5min respectively. Meanwhile, the effect of moisture on NO_2 gas sensing was considered (**Fig. 13**e and f). They also proposed a plausible mechanism for the formation of ZnO/PANI heterojunction microstructure (**Fig. 15**a) and a corresponding NO_2 sensing mechanism model (**Fig. 15**b).

3.3. Inorganic adding

Inorganics such as CuO [113] and NiO [114] occasionally are adopt to act as the second components to reduce the operating temperature of ZnO based gas sensors. The formed heterojunction or synergic effect is responsible for the room-temperature gas sensing. For instance, Krishnakumar Lokesh et al. [114] successfully prepared the n-ZnO/p-NiO nanofibers (**Fig. 16**a and b) using electrospinning method to employ as room temperature ammonia sensor. The nanostructure n-ZnO/p-NiO heterostructure exhibited the response of 67 for 250 ppm of ammonia at room temperature (**Fig. 16**c) and were highly selective to ammonia (**Fig. 16**d). Xinghua Chang et al. [115] reported that $CdSO_4$ modified ZnO sensor working at room temperature showed high sensitivity to formaldehyde with detection limit lower than 1 ppm. They attributed the high sensitivity toward formaldehyde to the synergic effect of Cd^{2+} and SO_4^{2-}.

In a word, doping additives increases the charge carrier concentration, and also decreases the activation energy of surface sensing reaction, finally reducing the operating temperature of ZnO based gas sensors. Compared with simple surface modification of pure ZnO nanostructure, generally speaking, additives doping especially metal adding sharply promotes the room-temperature gas sensing properties of ZnO.

4. Light activation

With the exception of surface modification based pure ZnO and additive adding, light activation is a promising strategy instead of thermal activation to realize room-temperature gas sensing of ZnO sensors. **Table 5** summarizes the room-temperature

gas sensing performances of ZnO based gas sensors under UV or visible-light illumination.

4.1. UV activation

UV as excitation energy has drawn a tremendous attention to reducing the operating temperature of ZnO based gas sensors [14, 36]. When ZnO based gas sensors are positioned in dark environment, the chemisorbed oxygen species reveal less quantity and are difficult to remove from ZnO surface at room temperature [32, 36]. However, when the sensors are illuminated under UV light with the photon energy equal or higher than the band gap of ZnO (3.37eV), electrons from the valence band can be rapidly excited to the conduction band, generating plenty of photo-induced electron-hole pairs existing in ZnO[23, 69]. The maximum wavelength (λ_{max}) of UV light used for activation can be calculated as given in the following equation,

$$\lambda_{max} \leq hc/E_g \approx 368 \text{ nm} \quad (1)$$

where h is the Planck's constant (4.14×10^{-15} eV·s), c is the velocity of light (3.00×10^{8} m·s^{-1}) and E_g is the band gap of ZnO (3.37eV). As shown in **Fig. 17**, owing to the built-in electric field, the photo-induced electrons will diffuse toward the inside of ZnO, whereas the photo-induced holes will migrate to the surface and react with the chemisorbed oxygen species, causing the desorption of oxygen from ZnO surface [74, 124-126]. Meanwhile, additional photo-induced oxygen species are generated through the interaction between the oxygen molecules and the active photoelectrons remaining on ZnO surface, which are bound to the surface weakly as compared to chemisorbed

oxygen species [31, 32]. As a consequence, unpaired electrons left in the conduction channel result in the diminishment of depletion layer and a rapid increase in current of ZnO based gas sensors, despite a little increase of ZnO resistance caused by the interaction between some photo-induced electrons and ambient oxygen molecules [13, 32]. Upon exposure to target gas, the change in resistance of ZnO based gas sensors accompanying the adsorption and desorption of surface molecules will increase under UV activation. As a consequence, ZnO based gas sensors present a high sensor response and a fast response-recovery speed under UV illumination at lower operating temperature [36, 127-129].

It is necessary to note that the photo-activated room-temperature properties are also affected by the wavelength and intensity of UV light [31, 36, 128]. **Fig. 18**a showed dynamic responses of ZnS-core/ZnO-shell nanowires to 5 ppm NO_2 gas at room temperature under UV illumination at different intensities. The responses of the core-shell nanowires increased from 116 to 1180% with increasing UV illumination intensity from 0 to 1.2 mW/cm^2. In contrast, the response of the core-shell nanowires to NO_2 gas was obviously stronger under UV (365 nm) illumination than in the dark and far stronger under shorter wavelength-UV (254 nm) illumination (**Fig. 18**b). Higher intensity and shorter wavelength of UV with larger excitation energy may increase the number of electron-hole pairs, which significantly increase the charge carrier concentration, resulting to room-temperature operation.

Ekasiddh Wongrat et al. [13] fabricated the sensors based on bare-ZnO and ZnO decorated with gold nanoparticles (ZnO:AuNPs) at different sputtering times. They

applied the co-technique including ZnO with AuNPs decoration and UV illumination to reduce the operating temperature and enhance the sensor response of ZnO sensors. The ethanol sensing properties were measured under dark and different UV illumination intensities. As can be seen from **Fig. 19**a, the sensor response of a representative S06 sensor (ZnO:AuNPs at the sputtering time of 6 s) to 1000 ppm ethanol vapor at room temperature was investigated in order to evaluate the UV illumination intensities effect. The comparison of the room-temperature sensor response between the bare-ZnO (S00) and the S06 sensor was shown in **Fig. 19**b. It was observed that, S00 or S06 sensor, the ethanol sensing enhancement was achieved under UV illumination in varying degrees, which was explained by the spill-over effect and UV activation. **Fig. 19**c and d showed the surface reaction mechanism of sensors based on bare-ZnO and ZnO:AuNPs under dark condition and UV illumination.

4.2. Visible-light activation

It is generally known that UV source is power-hungry, expensive and harmful to human health. Further still, UV may resolve certain materials and target gases [23]. On the contrary, visible-light source is inexpensive and environmental friendly [35, 130].

It should keep in mind that the photo-induced electron-hole pairs are produced when the excitation energy is equal or higher than the wide band gap of ZnO. Namely, the wavelength of UV should be less than about 368nm. However, the wavelength of visible light is in the range of 400-760 nm, the direct generation of electron-hole pairs has been ruled out. Given this, the method of introducing dopants including the narrow

band-gap semiconductors like CdS [23, 69] and metals like Au [35, 42, 131] to ZnO is practical to indirectly produce electron-hole pairs, with an aim to reduce the operating temperature of ZnO based gas sensors.

As shown in **Fig. 20**a, when the ZnO based sensing layer incorporated with CdS is exposed to visible light, electron-hole pairs are formed and then electrons from the excited narrow band-gap semiconductor will be transferred to the conduction band of ZnO. The electron concentration of ZnO increases rapidly, resulting in a thinner depletion layer with lower resistance. Accordingly, the obtained sensors show higher response at room temperature under visible light as compared to the case in dark condition. Actually, the research of ZnO combined with other narrow band-gap semiconductors such as Bi_2S_3 [132] and PbS [133] is still rare.

Another situation, ZnO is decorated with metals like Au. In addition to the catalysis of Au nanoparticles, the localized surface plasmon response (LSPR) effect plays a vital role in enhancement of room-temperature gas sensing properties of ZnO based gas sensors shown in **Fig. 20**b. Massive electrons oscillate on Au surface owing to the resonance when visible light interacts with plasmons, producing hot electrons and an electromagnetic field [35, 42, 131]. Then a large number of plasmon-induced hot electrons will be injected into the conduction band over the Schottky barrier, leading to an increase in electron concentration of ZnO. Additional visible light-induced oxygen species are formed by the interaction of oxygen molecules with hot electrons. These visible light-induced oxygen species are also weakly bound to ZnO, which

eventually benefit for the room-temperature gas sensing enhancement, in comparison with the response in darkroom.

In brief, UV-assisted or visible light-assisted excitation could contribute to room temperature gas sensing of ZnO based gas sensors by generating photo-induced electron-hole pairs. As far as we know, however, there are almost no comparative study of UV-assisted and light-assisted excitation on gas sensing properties of ZnO, and related work of other semiconducting metal oxide like TiO_2 has been reported [134].

5. Conclusions

Gas sensors are rapidly developing toward the direction of miniaturization and low power consumption, and room-temperature operation can exactly make for it. So tremendous progresses for reducing operating temperature of ZnO based gas sensors to room temperature also have been made in recent years as briefly summarized in **Table 3-5**. To our delight, it makes considerable headway in sharply facilitating room-temperature gas sensing performances by surface modification based pure ZnO, additive doping, UV or visible-light irradiation mentioned above. Small grain size, high effective specific area, and density of defects and porosity are responsible for the enhancement of pure ZnO gas sensing. Nevertheless, simple surface modification can only reduce operating temperature to a certain extent and hardly realize high room-temperature gas sensing. In light of the above summarization, we discover that additive doping such as metal, conducting polymer and inorganic adding is an effective way to achieve room-temperature gas sensing of ZnO based gas sensors. Especially the

functionalization of metal dopants promotes the superior room-temperature gas sensing properties caused by increased charge carrier concentration and decreased activation energy. This is to point the way to develop higher room-temperature gas sensing of ZnO based gas sensors and even other gas sensors. However, it must be said that metal additives in-turn increase cost of the sensors at the same time. In addition, UV or visible-light irradiation is another route to reduce the operating temperature of ZnO gas sensors instead of electric heating. A host of photo-induced electrons under light illumination improve the electric behaviors, leading to room-temperature gas sensing of ZnO based gas sensors.

6. Outlook

Currently, we are all confronted with a challenge of generally higher operating temperature of ZnO based gas sensors. Although significant progress of room-temperature operation of ZnO based gas sensors has been witnessed, research endeavors still should be further done. For surface morphological modification, novel ZnO nanostructures such as unique three-dimension hierarchical architectures with higher sensing capabilities could be synthesized via optimizing process parameters. In addition, additive doping particularly the metal adding is a fantastic method to reduce the operating temperature of ZnO gas sensors. Based on our elaborate summarization, it is found that most of previous studies are nearly focused on the mono-metal doping. There are few reports about multi-metallic doping, which may be a good research direction in the near future. Its detailed mechanism also need to be further excavated. Besides, for light irradiation, a further comparative study of UV and visible light

illumination on gas sensing of ZnO could be carried out to critically analyze their detailed difference.

For room-temperature gas sensing material investigations, in fact, the co-effect of combination of several different strategies has been used, but it is still rarely reported, particularly integrating the functionalization of metal dopants with other techniques. Finally, we hope our work can open up a new avenue to further exploration on higher room-temperature gas sensing of ZnO and even other sensing materials.

Acknowledgements

This work was supported by Chongqing Research Program of Basic Research and Frontier Technology (No. cstc2016jcyjA0006)

References

[1] S.P. Patil, V.L. Patil, S.S. Shendage, N.S. Harale, S.A. Vanalakar, J.H. Kim, et al., Spray pyrolyzed indium oxide thick films as NO_2 gas sensor, Ceram. Int. 42 (2016) 16160-16168.

[2] L. Zhu, W. Zeng, A novel coral rock-like ZnO and its gas sensing. Mater. Lett. 209 (2017) 244-246.

[3] C. Wang, W. Zeng, New insights into multi-hierarchical nanostructures with size-controllable blocking units for their gas sensing performance, J. Mater. Sci.: Mater. Electron. 28 (2017) 10847-10852.

[4] Y.H. Navale, S.T. Navale, N.S. Ramgir, F.J. Stadler, S.K. Gupta, D.K. Aswal, et al., Zinc oxide hierarchical nanostructures as potential NO_2 sensors, Sens. Actuators B: Chem. 251 (2017) 551-563.

[5] J. Jonca, J. Harmel, L. Joanny, A. Ryzhikov, M.L. Kahn, P. Fau, B. Chaudret, et al., Au/MO_x (M = Zn, Ti) nanocomposites as highly efficient catalytic filters for chemical gas sensing at room temperature and in humid atmosphere, Sens. Actuators B: Chem. 249 (2017) 357-363.

[6] C.-L. Hsu, L.-F. Chang, T.-J. Hsueh, Light-activated humidity and gas sensing by ZnO nanowires grown on LED at room temperature, Sens. Actuators B: Chem. 249 (2017) 265-277.

[7] P. Rai, Y.-S. Kim, H.-M. Song, M.-K. Song, Y.-T. Yu, The role of gold catalyst on the sensing behavior of ZnO nanorods for CO and NO_2 gases, Sens. Actuators B: Chem. 165 (2012) 133-142.

[8] Z.L. Wang, Splendid one-dimensional nanostructures of zinc oxide: A new nanomaterial family for nanotechnology, Acs Nano. 2 (2008) 1987-1992.

[9] J. Zheng, Z.-Y. Jiang, Q. Kuang, Z.-X. Xie, R.-B. Huang, L.-S. Zheng, Shape-controlled

fabrication of porous ZnO architectures and their photocatalytic properties, J. Solid State Chem. 182 (2009) 115-121.

[10] S. Kundu, U. Nithiyanantham, DNA-mediated fast synthesis of shape-selective ZnO nanostructures and their potential applications in catalysis and dye-sensitized solar cells, Ind. Eng. Chem. Res. 53 (2014) 13667-13679.

[11] R. Sankar Ganesh, E. Durgadevi, M. Navaneethan, V.L. Patil, S. Ponnusamy, C. Muthamizhchelvan, et al., Low temperature ammonia gas sensor based on Mn-doped ZnO nanoparticle decorated microspheres, J. Alloy. Compd. 721 (2017) 182-190.

[12] M. Das, D. Sarkar, One-pot synthesis of zinc oxide-polyaniline nanocomposite for fabrication of efficient room temperature ammonia gas sensor, Ceram. Int. 43 (2017) 11123-11131.

[13] E. Wongrat, N. Chanlek, C. Chueaiarrom, B. Samransuksamer, N. Hongsith, S. Choopun, Low temperature ethanol response enhancement of ZnO nanostructures sensor decorated with gold nanoparticles exposed to UV illumination, Sens. Actuators A: Phys. 251 (2016) 188-197.

[14] J. Cui, J. Jiang, L. Shi, F. Zhao, D. Wang, Y. Lin, et al., The role of Ni doping on photoelectric gas-sensing properties of ZnO nanofibers to HCHO at room-temperature, RSC Adv. 6 (2016) 78257-78263.

[15] Z. Jing, J. Zhan, Fabrication and gas-sensing properties of porous ZnO nanoplates, Adv. Mater. 20 (2008) 4547-4551.

[16] C. Liu, L. Zhao, B. Wang, P. Sun, Q. Wang, Y. Gao, et al., Acetone gas sensor based on NiO/ZnO hollow spheres: Fast response and recovery, and low (ppb) detection limit, J. Colloid Interf. Sci. 495 (2017) 207-215.

[17] R.K. Sonker, S.R. Sabhajeet, S. Singh, B.C. Yadav, Synthesis of ZnO nanopetals and its

application as NO_2 gas sensor, Mater. Lett. 152 (2015) 189-191.

[18] L. Yu, F. Guo, S. Liu, B. Yang, Y. Jiang, L. Qi, X. Fan, Both oxygen vacancies defects and porosity facilitated NO_2 gas sensing response in 2D ZnO nanowalls at room temperature, J. Alloy. Compd. 682 (2016) 352-356.

[19] Y. Cai, H. Fan, One-step self-assembly economical synthesis of hierarchical ZnO nanocrystals and their gas-sensing properties, CrystEngComm 15 (2013) 9148.

[20] J. Guo, J. Zhang, M. Zhu, D. Ju, H. Xu, B. Cao, High-performance gas sensor based on ZnO nanowires functionalized by Au nanoparticles, Sens. Actuators B: Chem. 199 (2014) 339-345.

[21] P. Patil, G. Gaikwad, D.R. Patil, J. Naik, Synthesis of 1-D ZnO nanorods and polypyrrole/1-D ZnO nanocomposites for photocatalysis and gas sensor applications, Bull. Mater. Sci. 39 (2016) 655-665.

[22] J. Xu, Y.a. Shun, Q. Pan, J. Qin, Sensing characteristics of double layer film of ZnO, Sens. Actuators B: Chem. 66 (2000) 161-163.

[23] X. Geng, C. Zhang, M. Debliquy, Cadmium sulfide activated zinc oxide coatings deposited by liquid plasma spray for room temperature nitrogen dioxide detection under visible light illumination, Ceram. Int. 42 (2016) 4845-4852.

[24] L. Zhu, W. Zeng, A novel coral rock-like ZnO and its gas sensing, Mater. Lett. 209 (2017) 244-246.

[25] L. Zhu, Y. Li, W. Zeng, Hydrothermal synthesis of hierarchical flower-like ZnO nanostructure and its enhanced ethanol gas-sensing properties, Appl. Surf. Sci. 427 (2018) 281-287.

[26] J. Xu, Q. Pan, Y. Shun, Z. Tian, Grain size control and gas sensing properties of ZnO gas sensor, Sens. Actuators B: Chem. 66 (2000) 279.

[27] X. Liu, J. Sun, X. Zhang, Novel 3D graphene aerogel-ZnO composites as efficient detection for NO2 at room temperature, Sens. Actuators B: Chem. 211 (2015) 220-226.

[28] J.F. Chang, H.H. Kuo, I.C. Leu, M.H. Hon, The effects of thickness and operation temperature on ZnO: Al thin film CO gas sensor, Sens. Actuators B: Chem. 84 (2002) 258-264.

[29] Z.S. Hosseini, A.I. zad, A. Mortezaali, Room temperature H_2S gas sensor based on rather aligned ZnO nanorods with flower-like structures, Sens. Actuators B: Chem. 207 (2015) 865-871.

[30] G. Korotcenkov, B.K. Cho, The role of grain size on the thermal instability of nanostructured metal oxides used in gas sensor applications and approaches for grain-size stabilization, Prog. Cryst. Growth Charact. Mater. 58 (2012) 167-208.

[31] S. Park, S. An, Y. Mun, C. Lee, UV-enhanced NO_2 gas sensing properties of SnO2-core/ZnO-shell nanowires at room temperature, ACS Appl. Mater. Interf. 5 (2013) 4285-4292.

[32] S.-W. Fan, A.K. Srivastava, V.P. Dravid, UV-activated room-temperature gas sensing mechanism of polycrystalline ZnO, Appl. Phys. Lett. 95 (2009) 142106.

[33] D.R. Miller, S.A. Akbar, P.A. Morris, Nanoscale metal oxide-based heterojunctions for gas sensing: A review, Sens. Actuators B: Chem. 204 (2014) 250-272.

[34] D.E. Motaung, I. Kortidis, G.H. Mhlongo, M.-M. Duvenhage, H.C. Swart, G. Kiriakidis, S.S. Ray, Correlating the magnetism and gas sensing properties of Mn-doped ZnO films enhanced by UV irradiation, RSC Adv. 6 (2016) 26227-26238.

[35] Z.Q. Zheng, B. Wang, J.D. Yao, G.W. Yang, Light-controlled C2H2 gas sensing based on Au-ZnO nanowires with plasmon-enhanced sensitivity at room temperature, J. Mater. Chem. C 3 (2015) 7067-7074.

[36] S. Mishra, C. Ghanshyam, N. Ram, R.P. Bajpai, R.K. Bedi, Detection mechanism of metal oxide gas sensor under UV radiation, Sens. Actuators B: Chem. 97 (2004) 387-390.

[37] P. Sundara Venkatesh, P. Dharmaraj, V. Purushothaman, V. Ramakrishnan, K. Jeganathan, Point defects assisted NH3 gas sensing properties in ZnO nanostructures, Sens. Actuators B: Chem. 212 (2015) 10-17.

[38] P. Shankar, J.B. Rayappan, Racetrack effect on the dissimilar sensing response of ZnO thin film-an anisotropy of isotropy, ACS Appl. Mater. Interf. 8 (2016) 24924-24932.

[39] G.K. Mani, J.B.B. Rayappan, A highly selective and wide range ammonia sensor-Nanostructured ZnO:Co thin film, Mater. Sci. Eng. B 191 (2015) 41-50.

[40] G.K. Mani, J.B.B. Rayappan, A highly selective room temperature ammonia sensor using spray deposited zinc oxide thin film, Sens. Actuators B: Chem. 183 (2013) 459-466.

[41] G.K. Mani, J.B.B. Rayappan, Novel and facile synthesis of randomly interconnected ZnO nanoplatelets using spray pyrolysis and their room temperature sensing characteristics, Sens. Actuators B: Chem. 198 (2014) 125-133.

[42] A.L. Zou, Y. Qiu, J.J. Yu, B. Yin, G.Y. Cao, H.Q. Zhang, et al., Ethanol sensing with Au-modified ZnO microwires, Sens. Actuators B: Chem. 227 (2016) 65-72.

[43] P. Shankar, J.B.B. Rayappan, Gas sensing mechanism of metal oxides: The role of ambient atmosphere, type of semiconductor and gases-a review, Sci. Lett. J. 126 (2015) 1-18.

[44] P.K. Kannan, R. Saraswathi, J.B.B. Rayappan, A highly sensitive humidity sensor based on DC reactive magnetron sputtered zinc oxide thin film, Sens. Actuators A: Phys. 164 (2010) 8-14.

[45] M. Sinha, R. Mahapatra, B. Mondal, T. Maruyama, R. Ghosh, Ultrafast and reversible gas-

sensing properties of ZnO nanowire arrays grown by hydrothermal technique, J. Phys. Chem. C 120 (2016) 3019-3025.

[46] T. Tesfamichael, C. Cetin, C. Piloto, M. Arita, J. Bell, The effect of pressure and W-doping on the properties of ZnO thin films for NO_2 gas sensing, Appl. Surf. Sci. 357 (2015) 728-734.

[47] F. Fang, L. Bai, D. Song, H. Yang, X. Sun, H. Sun, et al., Ag-modified In_2O_3/ZnO nanobundles with high formaldehyde gas-sensing performance, Sensors (Basel) 15 (2015) 20086-20096.

[48] J. Zhang, X. Liu, G. Neri, N. Pinna, Nanostructured materials for room-temperature gas sensors, Adv. Mater. 28 (2016) 795-831.

[49] S. Liu, B. Yu, H. Zhang, T. Fei, T. Zhang, Enhancing NO_2 gas sensing performances at room temperature based on reduced graphene oxide-ZnO nanoparticles hybrids, Sens. Actuators B: Chem. 202 (2014) 272-278.

[50] H. Mu, Z. Zhang, X. Zhao, F. Liu, K. Wang, H. Xie, High sensitive formaldehyde graphene gas sensor modified by atomic layer deposition zinc oxide films, Appl. Phys. Lett. 105 (2014) 033107.

[51] H. Tai, Z. Yuan, W. Zheng, Z. Ye, C. Liu, X. Du, ZnO nanoparticles/reduced graphene oxide bilayer thin films for improved NH3-sensing performances at room temperature, Nanoscale Res. Lett. 11 (2016) 130.

[52] L. Zhu, Y. Li, W. Zeng, Enhanced ethanol sensing and mechanism of Cr-doped ZnO nanorods: Experimental and computational study, Ceram. Int. 43 (2017) 14873-14879.

[53] F. Fan, P. Tang, Y. Wang, Y. Feng, A. Chen, R. Luo, et al., Facile synthesis and gas sensing properties of tubular hierarchical ZnO self-assembled by porous nanosheets, Sens. Actuators B: Chem. 215 (2015) 231-240.

[54] R. Dhahri, M. Hjiri, L. El Mir, A. Bonavita, D. Iannazzo, M. Latino, et al., Gas sensing properties of Al-doped ZnO for UV-activated CO detection, J. Phys. D: Appl. Phys. 49 (2016) 135502.

[55] C. Zou, F. Liang, S. Xue, Synthesis and oxygen vacancy related NO_2 gas sensing properties of ZnO:Co nanorods arrays gown by a hydrothermal method, Appl. Surf. Sci. 353 (2015) 1061-1069.

[56] R. Dhahri, M. Hjiri, L.E. Mir, A. Bonavita, D. Iannazzo, S.G. Leonardi, et al., CO sensing properties under UV radiation of Ga-doped ZnO nanopowders, Appl. Surf. Sci. 355 (2015) 1321-1326.

[57] N.M. Vuong, N.D. Chinh, B.T. Huy, Y.I. Lee, CuO-decorated ZnO hierarchical nanostructures as efficient and established sensing materials for H_2S gas sensors, Sci. Rep. 6 (2016) 26736.

[58] Y. Cao, X. Zou, X. Wang, J. Qian, N. Bai, G.-D. Li, Effective detection of trace amount of explosive nitro-compounds by ZnO nanofibers with hollow structure, Sens. Actuators B: Chem. 232 (2016) 564-570.

[59] C.-F. Li, C.-Y. Hsu, Y.-Y. Li, NH3 sensing properties of ZnO thin films prepared via sol-gel method, J. Alloy. Compd. 606 (2014) 27-31.

[60] I. Rawal, Facial synthesis of hexagonal metal oxide nanoparticles for low temperature ammonia gas sensing applications, RSC Adv. 5 (2015) 4135-4142.

[61] J. Deng, Q. Fu, W. Luo, X. Tong, J. Xiong, Y. Hu, et al., Enhanced H2S gas sensing properties of undoped ZnO nanocrystalline films from QDs by low-temperature processing, Sens. Actuators B: Chem. 224 (2016) 153-158.

[62] A. Tamvakos, D. Calestani, D. Tamvakos, R. Mosca, D. Pullini, A. Pruna, Effect of grain-size

on the ethanol vapor sensing properties of room-temperature sputtered ZnO thin films, Microchim. Acta 182 (2015) 1991-1999.

[63] C. Li, Z. Du, H. Yu, T. Wang, Low-temperature sensing and high sensitivity of ZnO nanoneedles due to small size effect, Thin Solid Films 517 (2009) 5931-5934.

[64] A. Rothschild, Y. Komem, The effect of grain size on the sensitivity of nanocrystalline metal-oxide gas sensors, J. Appl. Phys. 95 (2004) 6374-6380.

[65] L. Shi, J. Cui, F. Zhao, D. Wang, T. Xie, Y. Lin, High-performance formaldehyde gas-sensors based on three dimensional center-hollow ZnO, Phys. Chem. Chem. Phys. 17 (2015) 31316-31323.

[66] B. Min, SnO_2 thin film gas sensor fabricated by ion beam deposition, Sens. Actuators B: Chem. 98 (2004) 239-246.

[67] G. Korotcenkov, B.K. Cho, Instability of metal oxide-based conductometric gas sensors and approaches to stability improvement (short survey), Sens. Actuators B: Chem. 156 (2011) 527.

[68] W. Guo, T. Liu, H. Zhang, R. Sun, Y. Chen, W. Zeng, et al., Gas-sensing performance enhancement in ZnO nanostructures by hierarchical morphology, Sens. Actuators B: Chem. 166-167 (2012) 492-499.

[69] X. Geng, J. You, C. Zhang, Microstructure and sensing properties of CdS-ZnO_{1-x} coatings deposited by liquid plasma spray and treated with hydrogen peroxide solution for nitrogen dioxide detection at room temperature, J. Alloy. Compd. 687 (2016) 286-293.

[70] J. Wang, X. Li, Y. Xia, S. Komarneni, H. Chen, J. Xu, et al., Hierarchical ZnO nanosheet-nanorod architectures for fabrication of Poly(3-hexylthiophene)/ZnO hybrid NO_2 sensor, ACS Appl. Mater. Interf. 8 (2016) 8600-8607.

[71] D. Acharyya, P. Bhattacharyya, Alcohol sensing performance of ZnO hexagonal nanotubes at low temperatures: A qualitative understanding, Sens. Actuators B: Chem. 228 (2016) 373-386.

[72] J. Cui, L. Shi, T. Xie, D. Wang, Y. Lin, UV-light illumination room temperature HCHO gas-sensing mechanism of ZnO with different nanostructures, Sens. Actuators B: Chem. 227 (2016) 220-226.

[73] L. Balakrishnan, S. Gokul Raj, S.R. Meher, K. Asokan, Z.C. Alex, Impact of 100 MeV Ag7+ SHI irradiation fluence and N incorporation on structural, optical, electrical and gas sensing properties of ZnO thin films, Appl. Phys. A 119 (2015) 1541-1553.

[74] S. Park, G.J. Sun, C. Jin, H.W. Kim, S. Lee, C. Lee, Synergistic effects of a combination of Cr_2O_3-functionalization and UV-Irradiation techniques on the ethanol gas sensing performance of ZnO nanorod gas sensors, ACS Appl. Mater. Interf. 8 (2016) 2805-2811.

[75] S.M. Mohammad, Z. Hassan, R.A. Talib, N.M. Ahmed, M.A. Al-Azawi, N.M. Abd-Alghafour, et al., Fabrication of a highly flexible low-cost H_2 gas sensor using ZnO nanorods grown on an ultra-thin nylon substrate, J. Mater. Sci.: Mater. Electron. 27 (2016) 9461-9469.

[76] G.H. Mhlongo, K. Shingange, Z.P. Tshabalala, B.P. Dhonge, F.A. Mahmoud, B.W. Mwakikunga, et al., Room temperature ferromagnetism and gas sensing in ZnO nanostructures: Influence of intrinsic defects and Mn, Co, Cu doping, Appl. Surf. Sci. 390 (2016) 804-815.

[77] G. Qi, X. Lu, Z. Yuan, Improved H_2S gas sensing properties of ZnO nanorods via decoration of nano-porous SiO_2 thin layers, RSC Adv. 6 (2016) 45660-45663.

[78] G.K. Mani, J.B.B. Rayappan, Facile synthesis of ZnO nanostructures by spray pyrolysis technique and its application as highly selective H2S sensor, Mater. Lett. 158 (2015) 373-376.

[79] J.J. Hassan, M.A. Mahdi, C.W. Chin, H. Abu-Hassan, Z. Hassan, Room temperature hydrogen gas sensor based on ZnO nanorod arrays grown on a SiO_2/Si substrate via a microwave-assisted chemical solution method, J. Alloy. Compd. 546 (2013) 107-111.

[80] K. Yadav, S.K. Gahlaut, B.R. Mehta, J.P. Singh, Photoluminescence based H_2 and O_2 gas sensing by ZnO nanowires, Appl. Phys. Lett. 108 (2016) 071602.

[81] T.Y. Tiong, C.F. Dee, A.A. Hamzah, B.Y. Majlis, S. Abdul Rahman, Enhancement of CuO and ZnO nanowires methanol sensing properties with diode-based structure, Sens. Actuators B: Chem. 202 (2014) 1322-1332.

[82] N. Kumar, A.K. Srivastava, R. Nath, B.K. Gupta, G.D. Varma, Probing the highly efficient room temperature ammonia gas sensing properties of a luminescent ZnO nanowire array prepared via an AAO-assisted template route, Dalton Trans. 43 (2014) 5713-5720.

[83] M. Kaur, S. Kailasaganapathi, N. Ramgir, N. Datta, S. Kumar, A.K. Debnath, et al., Gas dependent sensing mechanism in ZnO nanobelt sensor, Appl. Surf. Sci. 394 (2017) 258-266.

[84] J.Y. Lin, Z.X. Chen, X.L. He, W.M. Xie, Detection of H_2S at room temperature using ZnO sensors based on Hall Effect, Int. J. Electrochem. Sci. (2017) 6465-6476.

[85] M. Chitra, K. Uthayarani, N. Rajasekaran, N. Neelakandeswari, E.K. Girija, D.P. Padiyan, Rice husk templated mesoporous ZnO nanostructures for ethanol sensing at room temperature, Chinese Phys. Lett. 32 (2015) 078101.

[86] X. Pan, X. Zhao, Ultra-high sensitivity zinc oxide nanocombs for on-chip room temperature carbon monoxide sensing, Sensors (Basel) 15 (2015) 8919-8930.

[87] N. Zhang, K. Yu, Q. Li, Z.Q. Zhu, Q. Wan, Room-temperature high-sensitivity H_2S gas sensor based on dendritic ZnO nanostructures with macroscale in appearance, J. Appl. Phys. 103

(2008) 104305.

[88] B. Zhang, M. Li, Z. Song, H. Kan, H. Yu, Q. Liu, et al., Sensitive H_2S gas sensors employing colloidal zinc oxide quantum dots, Sens. Actuators B: Chem. 249 (2017) 558-563.

[89] M. Vanaraja, K. Muthukrishnan, S. Boomadevi, R.K. Karn, V. Singh, P.K. Singh, et al., Dip coated nanostructured ZnO thin film: Synthesis and application, Ceram. Int. 42 (2016) 4413-4420.

[90] K. Muthukrishnan, M. Vanaraja, S. Boomadevi, R.K. Karn, V. Singh, P.K. Singh, et al., Studies on acetone sensing characteristics of ZnO thin film prepared by sol-gel dip coating, J. Alloy. Compd. 673 (2016) 138-143.

[91] P. Dhivya, M. Sridharan, Nanostructured ZnO films for room temperature ammonia sensing, J. Electron. Mater. 43 (2014) 3211-3216.

[92] K. Vijayalakshmi, D. Gopalakrishna, Influence of pyrolytic temperature on the properties of ZnO films optimized for H_2 sensing application, J. Mater. Sci.: Mater. Electron. 25 (2014) 2253-2260.

[93] K. Shingange, Z.P. Tshabalala, O.M. Ntwaeaborwa, D.E. Motaung, G.H. Mhlongo, Highly selective NH3 gas sensor based on Au loaded ZnO nanostructures prepared using microwave-assisted method, J. Colloid Interf. Sci. 479 (2016) 127-138.

[94] F.-C. Chung, Z. Zhu, P.-Y. Luo, R.-J. Wu, W. Li, Au@ZnO core-shell structure for gaseous formaldehyde sensing at room temperature, Sens. Actuators B: Chem. 199 (2014) 314-319.

[95] N.S. Ramgir, P.K. Sharma, N. Datta, M. Kaur, A.K. Debnath, D.K. Aswal, et al., Room temperature H2S sensor based on Au modified ZnO nanowires, Sens. Actuators B: Chem. 186 (2013) 718-726.

[96] Z.-Y. Zhao, M.-H. Wang, T.-T. Liu, Tribulus terrestris leaf extract assisted green synthesis and gas sensing properties of Ag-coated ZnO nanoparticles, Mater. Lett. 158 (2015) 274-277.

[97] D.-T. Phan, G.-S. Chung, Effects of different morphologies of ZnO films on hydrogen sensing properties, J. Electroceram. 32 (2014) 353-360.

[98] G.K. Mani, J.B.B. Rayappan, ZnO nanoarchitectures: Ultrahigh sensitive room temperature acetaldehyde sensor, Sens. Actuators B: Chem. 223 (2016) 343-351.

[99] U.T. Nakate, P. Patil, R.N. Bulakhe, C.D. Lokhande, S.N. Kale, M. Naushad, et al., Sprayed zinc oxide films: Ultra-violet light-induced reversible surface wettability and platinum-sensitization-assisted improved liquefied petroleum gas response, J. Colloid Interf. Sci. 480 (2016) 109-117.

[100] M.E. Franke, T.J. Koplin, U. Simon, Metal and metal oxide nanoparticles in chemiresistors: does the nanoscale matter?, Small 2 (2006) 36-50.

[101] Z.S. Hosseini, A. Mortezaali, A. Iraji zad, S. Fardindoost, Sensitive and selective room temperature H_2S gas sensor based on Au sensitized vertical ZnO nanorods with flower-like structures, J. Alloy. Compd. 628 (2015) 222-229.

[102] G.K. Mani, J.B.B. Rayappan, Influence of copper doping on structural, optical and sensing properties of spray deposited zinc oxide thin films, J. Alloy. Compd. 582 (2014) 414-419.

[103] J. Iqbal, T. Jan, Y. Ronghai, Effect of Co doping on morphology, optical and magnetic properties of ZnO 1-D nanostructures, J. Mater. Sci.: Mater. Electron. 24 (2013) 4393-4398.

[104] L. Zhu, W. Zeng, Hydrothermal synthesis of hierarchical flower-like ZnO nanostructure and its enhanced ethanol gas-sensing properties, Appl. Surf. Sci. 427 (2018) 281-287.

[105] R.K. Sonker, B.C. Yadav, A. Sharma, M. Tomar, V. Gupta, Experimental investigations on

NO_2 sensing of pure ZnO and PANI-ZnO composite thin films, RSC Adv. 6 (2016) 56149-56158.

[106] A. Gusain, N.J. Joshi, P.V. Varde, D.K. Aswal, Flexible NO gas sensor based on conducting polymer poly[N-9′-heptadecanyl-2,7-carbazole-alt-5,5-(4′,7′-di-2-thienyl-2′,1′,3′-benzothiadiazole)] (PCDTBT), Sens. Actuators B: Chem. 239 (2017) 734-745.

[107] K. Dunst, J. Karczewski, P. Jasiński, Nitrogen dioxide sensing properties of PEDOT polymer films, Sensor. Actuators B: Chem. 247 (2017) 108-113.

[108] X. Wang, S. Meng, W. Ma, J. Pionteck, M. Gnanaseelan, Z. Zhou, et al., Fabrication and gas sensing behavior of poly(3,4-ethylenedioxythiophene) coated polypropylene fiber with engineered interface, React. Funct. Polym. 112 (2017) 74-80.

[109] M. Shaik, V.K. Rao, A.K. Sinha, K.S.R.C. Murthy, R. Jain, Sensitive detection of nitrogen dioxide gas at room temperature using poly(3,4-ethylenedioxythiophene) nanotubes, J. Environ. Chem. Eng. 3 (2015) 1947-1952.

[110] S. Park, C. Park, H. Yoon, Chemo-electrical gas sensors based on conducting polymer hybrids, Polymers 9 (2017) 155.

[111] H. Bai, G. Shi, Gas sensors based on conducting polymers, Sensors 7 (2007) 267-307.

[112] M.R. Alenezi, S.J. Henley, N.G. Emerson, S.R. Silva, From 1D and 2D ZnO nanostructures to 3D hierarchical structures with enhanced gas sensing properties, Nanoscale 6 (2014) 235-247.

[113] X. Liu, B. Du, Y. Sun, M. Yu, Y. Yin, W. Tang, et al., M.N. Ashfold, Sensitive room temperature photoluminescence-based sensing of H_2S with novel CuO-ZnO nanorods, ACS Appl. Mater. Interf. 8 (2016) 16379-16385.

[114] K. Lokesh, G. Kavitha, E. Manikandan, G.K. Mani, K. Kaviyarasu, J.B.B. Rayappan, et al., Effective ammonia detection using n-ZnO/p-NiO heterostructured nanofibers, IEEE Sensors J. 16 (2016) 2477-2483.

[115] X. Chang, M. Peng, J. Yang, T. Wang, Y. liu, J. Zheng, X. Li, A miniature room temperature formaldehyde sensor with high sensitivity and selectivity using $CdSO_4$ modified ZnO nanoparticles, RSC Adv. 5 (2015) 75098-75104.

[116] S. Arunkumar, T. Hou, Y.-B. Kim, B. Choi, S.H. Park, S. Jung, et al., Au decorated ZnO hierarchical architectures: Facile synthesis, tunable morphology and enhanced CO detection at room temperature, Sens. Actuators B: Chem. 243 (2017) 990-1001.

[117] A.J. Kulandaisamy, J.R. Reddy, P. Srinivasan, K.J. Babu, G.K. Mani, P. Shankar, et al., Room temperature ammonia sensing properties of ZnO thin films grown by spray pyrolysis: Effect of Mg doping, J. Alloy. Compd. 688 (2016) 422-429.

[118] K. Vijayalakshmi, A. Renitta, Enhanced H_2 sensing performance presented by Mg doped ZnO films fabricated with a novel ITO seed layer, J. Mater. Sci.: Mater. Electron. 26 (2015) 3458-3465.

[119] K. Vijayalakshmi, K. Karthick, Growth of highly c-axis oriented Mg:ZnO nanorods on Al_2O_3 substrate towards high-performance H_2 sensing, Int. J. Hydrogen Energ. 39 (2014) 7165-7172.

[120] M. Hannas, A.K. Shafura, B.Y. Majlis, S.A.H. Alrokayan, H.A. Khan, M. Rusop, Study on doping effect of Sn doped ZnO thin films for gas sensing application, IEEE Student Conference on Reasearch and Development (2015) 435-440.

[121] K.S. Venkatesh, K. Vijayalakshmi, K. Karthick, S.R. Krishnamoorthi, N.S. Palani, R. Ilangovan, Fabrication of room temperature H_2 gas sensor using pure and La: ZnO with novel

nanocorn morphology prepared by sol-gel dip coating method, J. Mater. Sci.: Mater. Electron. 25 (2014) 4339-4347.

[122] R. Paulraj, P. Shankar, G.K. Mani, L. Nallathambi, J.B.B. Rayappan, Fabrication of PANI–ZnO nanocomposite thin film for room temperature methanol sensor, J. Mater. Sc.: Mater. Electron. 28 (2017) 10799-10805.

[123] F. Mosciano, G. Magna, A. Catini, G. Pomarico, E. Martinelli, R. Paolesse, et al., Room temperature CO detection by hybrid porphyrin-ZnO nanoparticles, Procedia Eng. 120 (2015) 71-74.

[124] H. Chen, Y. Liu, C. Xie, J. Wu, D. Zeng, Y. Liao, A comparative study on UV light activated porous TiO_2 and ZnO film sensors for gas sensing at room temperature, Ceram. Int. 38 (2012) 503-509.

[125] O. Lupan, V. Cretu, V. Postica, M. Ahmadi, B.R. Cuenya, L. Chow, I. Tiginyanu, B. Viana, T. Pauporté, R. Adelung, Silver-doped zinc oxide single nanowire multifunctional nanosensor with a significant enhancement in response, Sens. Actuators B: Chem. 223 (2016) 893-903.

[126] G. Cheng, X. Wu, B. Liu, B. Li, X. Zhang, Z. Du, ZnO nanowire Schottky barrier ultraviolet photodetector with high sensitivity and fast recovery speed, Appl. Phys. Lett. 99 (2011) 203105.

[127] Z.Q. Zheng, J.D. Yao, B. Wang, G.W. Yang, Light-controlling, flexible and transparent ethanol gas sensor based on ZnO nanoparticles for wearable devices, Sci. Rep. 5 (2015) 11070.

[128] S. Park, S. Kim, H. Ko, C. Lee, Light-enhanced gas sensing of ZnS-core/ZnO-shell nanowires at room temperature, J. Electroceram. 33 (2014) 75-81.

[129] A.C. Catto, L.F. da Silva, C. Ribeiro, S. Bernardini, K. Aguir, E. Longo, et al., An easy method

of preparing ozone gas sensors based on ZnO nanorods, RSC Adv. 5 (2015) 19528-19533.

[130] C. Zhang, J. Wang, M.-G. Olivier, M. Debliquy, Room temperature nitrogen dioxide sensors based on N719-dye sensitized amorphous zinc oxide sensors performed under visible-light illumination, Sens. Actuators B: Chem. 209 (2015) 69-77.

[131] N. Gogurla, A.K. Sinha, S. Santra, S. Manna, S.K. Ray, Multifunctional Au-ZnO plasmonic nanostructures for enhanced UV photodetector and room temperature NO sensing devices, Sci. Rep. 4 (2014) 6483.

[132] F. Liu, X. Shao, S. Yang, Bi_2S_3–ZnS/graphene complexes: Synthesis, characterization, and photoactivity for the decolorization of dyes under visible light, Mater. Sci. Semicond. Process. 34 (2015) 104-108.

[133] Y. Yang, W. Wang, Effects of incorporating PbS quantum dots in perovskite solar cells based on $CH_3NH_3PbI_3$, J. Power Sources 293 (2015) 577-584.

[134] Z. Wang, K. Wang, X. Peng, Q. Geng, X. Chen, W. Dai, X. Fu, X. Wang, Comparative study of ultraviolet light and visible light on the photo-assisted conductivity and gas sensing property of TiO_2, Sens. Actuators B: Chem. 248 (2017) 724-732.

[135] M. Kumar, R. Kumar, S. Rajamani, S. Ranwa, M. Fanetti, M. Valant, et al., Efficient room temperature hydrogen sensor based on UV-activated ZnO nano-network, Nanotechnology 28 (2017) 365502.

[136] Y. Mun, S. Park, S. An, C. Lee, H.W. Kim, NO_2 gas sensing properties of Au-functionalized porous ZnO nanosheets enhanced by UV irradiation, Ceramics International, 39 (2013) 8615-8622.

Biographies

Ling Zhu is currently a Master student at Chongqing University in China since 2017. Her research interest is in the development of micro fabrication and nanofabrication technologies.

Wen Zeng received his PhD degree in material science and engineering from the Chongqing University, China. He has been a visiting researcher in Tohoku University of Japan from 2009 to 2010. He is currently an associate professor in the College of Materials Science and Engineering at Chongqing University since 2012. His research interests are in the area of low-dimensional functional materials, semiconductor sensor and first principles calculation.

Figures & Tables

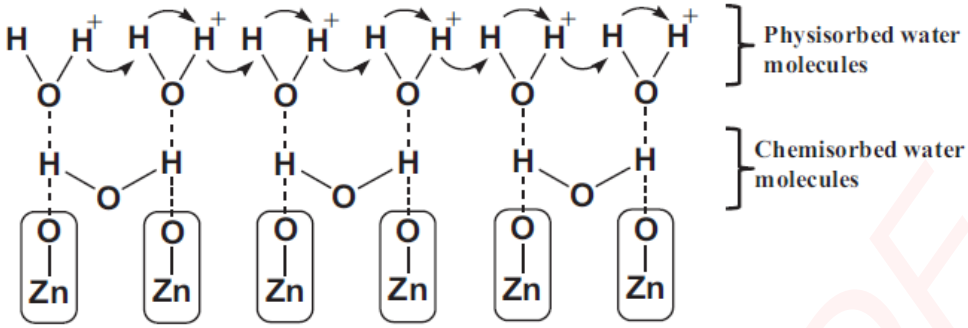

Fig. 1 Schematic representation of humidity sensing at ZnO [44].

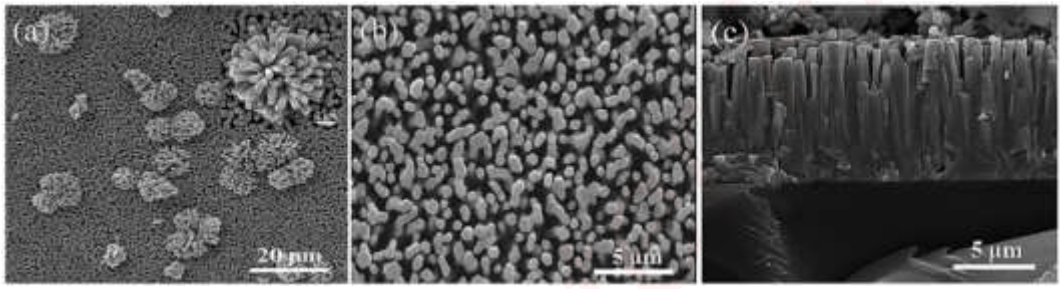

Fig. 2 SEM images of the vertically aligned ZnO nanorods with flower-like structures: (a, b) typical top view and (c) cross section. The inset is the magnified image of one of the flowers [29].

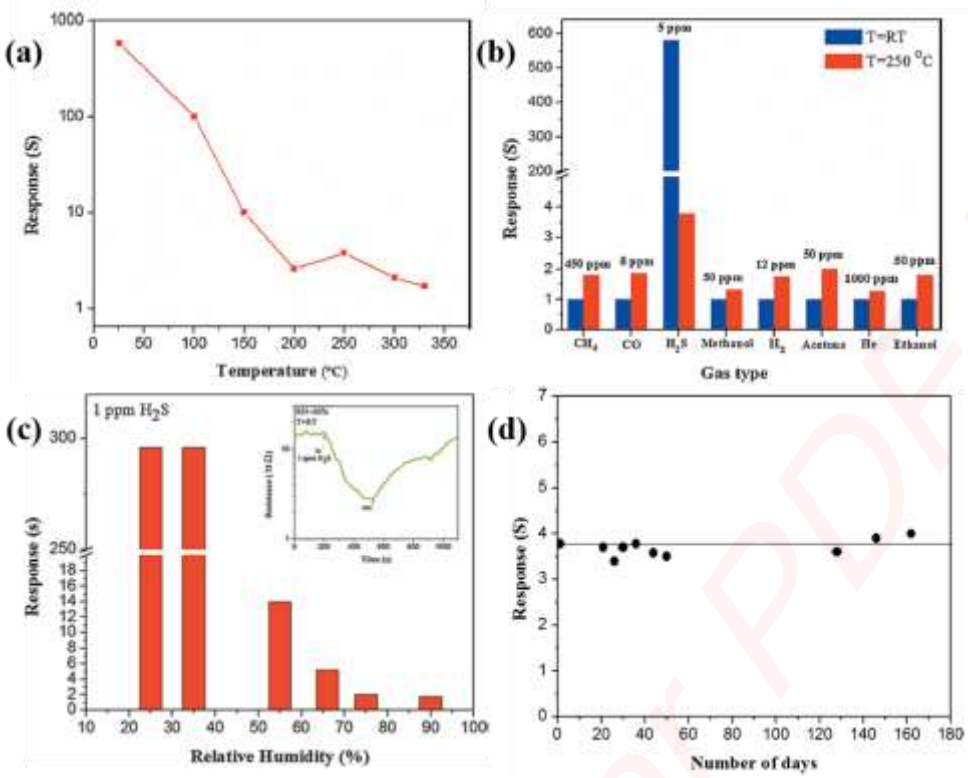

Fig. 3 (a) Response toward 5 ppm H_2S gas at various temperatures. (b) Response to different reducing gases at room temperature and 250°C. (c) Sensor response to 1 ppm H_2S gas in the presence of different relative humidifies at room temperature. The inset shows typical transient resistance response of the sensor toward 1 ppm H_2S at ~66% RH. (d) Variation in the sensor response to 5 ppm H_2S at 250°C for different periods of time [29].

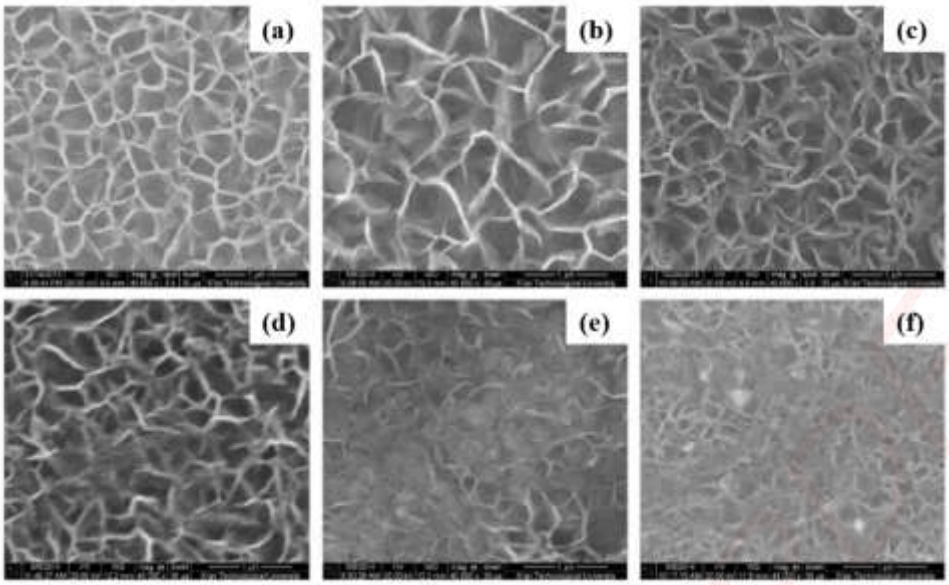

Fig. 4 The same magnification SEM images of ZnO nanowalls annealed at (a) 350°C, (b) 450°C, (c) 500°C, (d) 550°C, (e) 650°C, (f) 750°C [18].

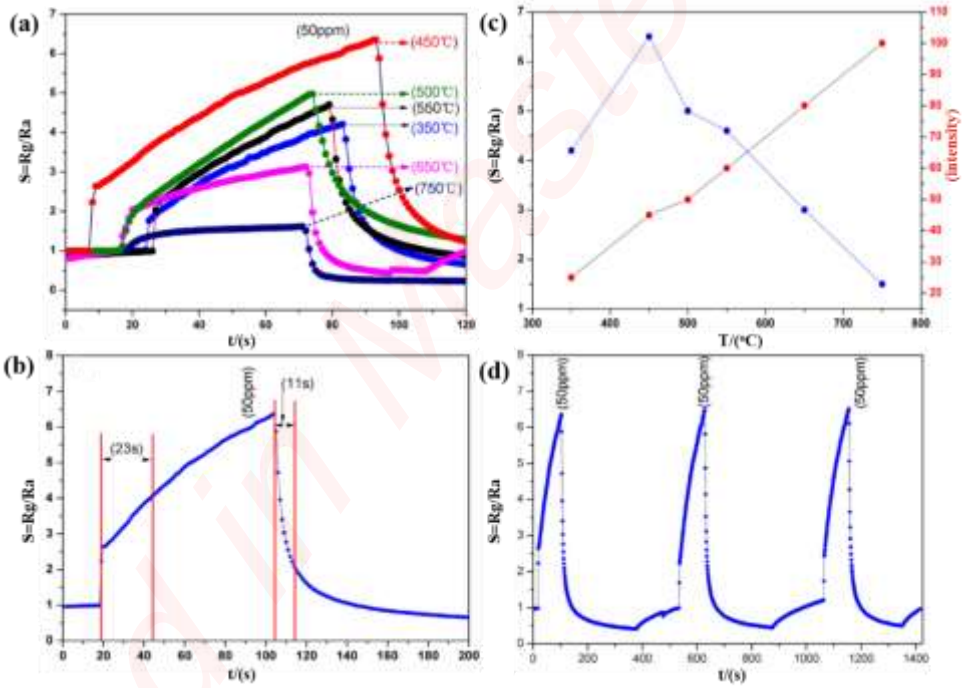

Fig. 5 (a) Typical response-recovery curves of ZnO nanowalls sensors to 50 ppm NO_2 at room temperature as a function of various annealing temperatures. (b) One circle response transients of ZnO-450°C gas sensors exposed to 50 ppm NO_2 at room temperature. (c) Relation between the oxygen vacancy defects and the gas response of ZnO nanowalls samples. (d)

Reproducibility of temporal response of ZnO-450°C exposed to 50 ppm NO_2 at room temperature [18].

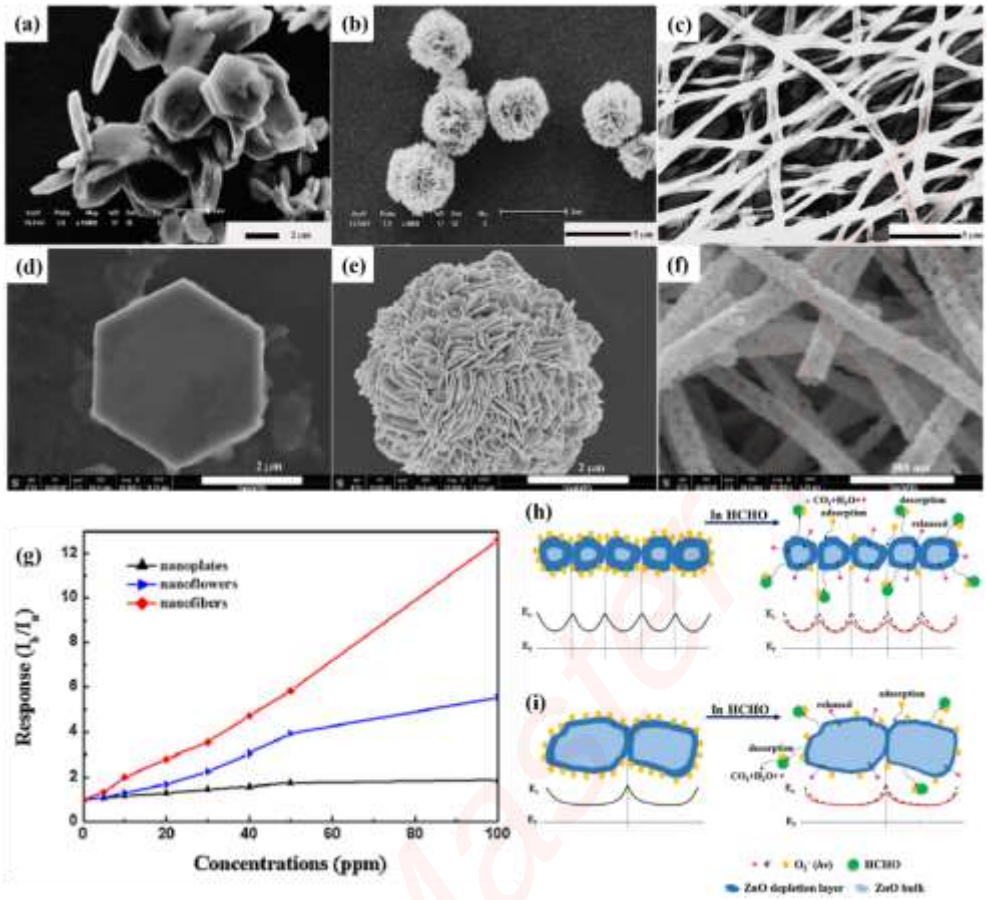

Fig. 6 SEM images of ZnO nanostructures: (a, d) nanoplates, (b, e) nanoflowers, (c, f) nanofibers. (g) Response of ZnO towards different HCHO concentration. Gas-sensing mechanism of (h) ZnO nanofibers, (i) ZnO nanoplates and nanoflowers to HCHO [72].

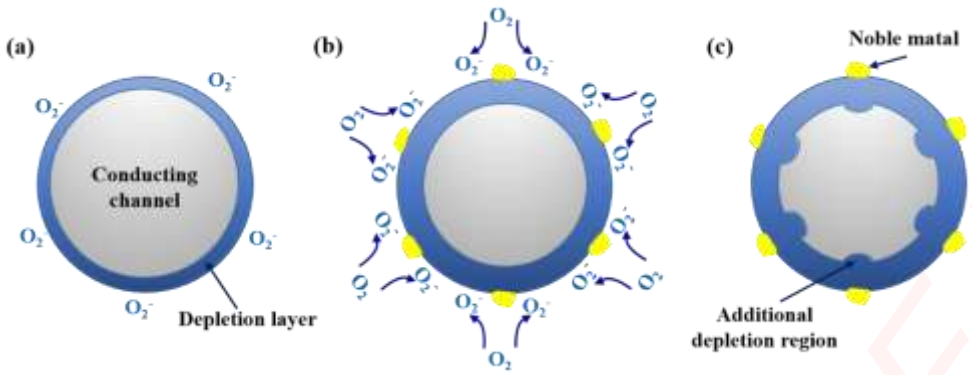

Fig. 7 (a) Schematic diagrams presenting depletion layer of unsensitized ZnO. Schematic illustration of (b) chemical effect (spill-over phenomenon) and (c) electric effect of noble metal sensitized ZnO.

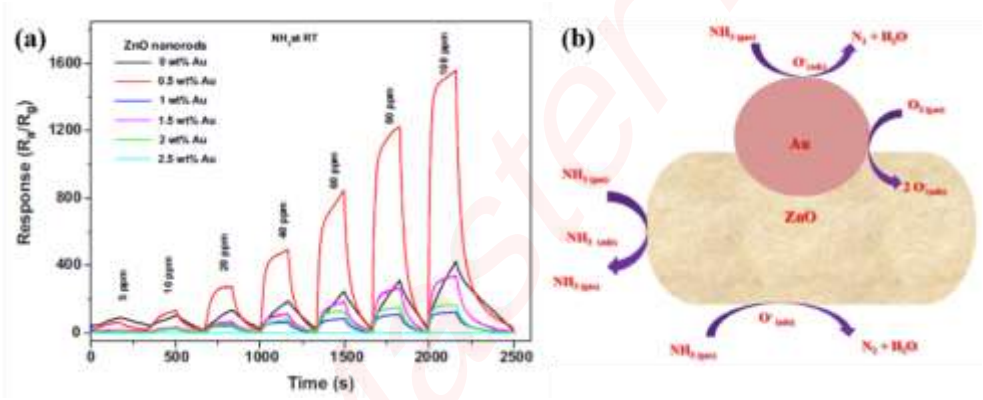

Fig. 8 (a) Response-recovery characteristics of pure and Au loaded ZnO sensors to various concentrations of NH_3 at room temperature. (b) Proposed NH_3 sensing mechanism for Au/ZnO nanorods [78].

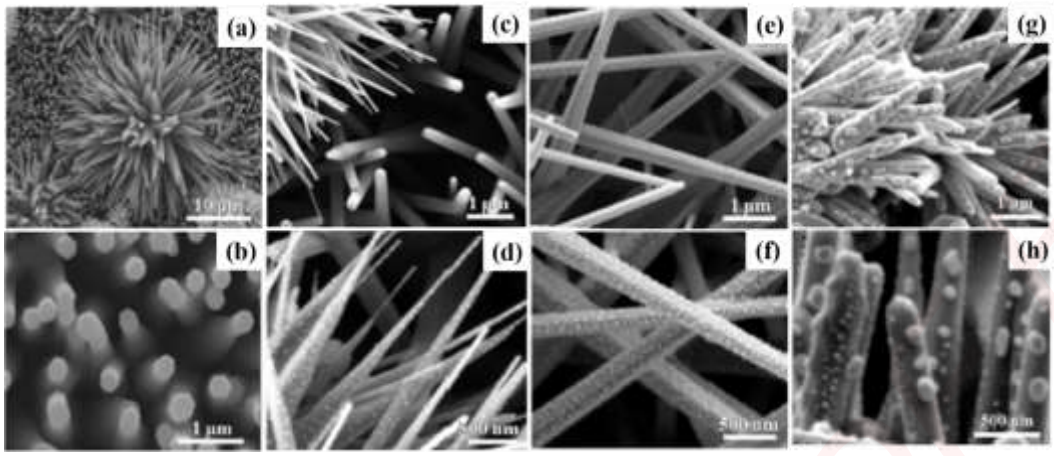

Fig. 9 SEM images of the grown ZnO rods with flower-like structures (a, b) without Au and with the different Au nominal thicknesses (c, d) Au (3 nm):ZnO (e, f) Au (6 nm):ZnO (g, h) Au (15 nm):ZnO [101].

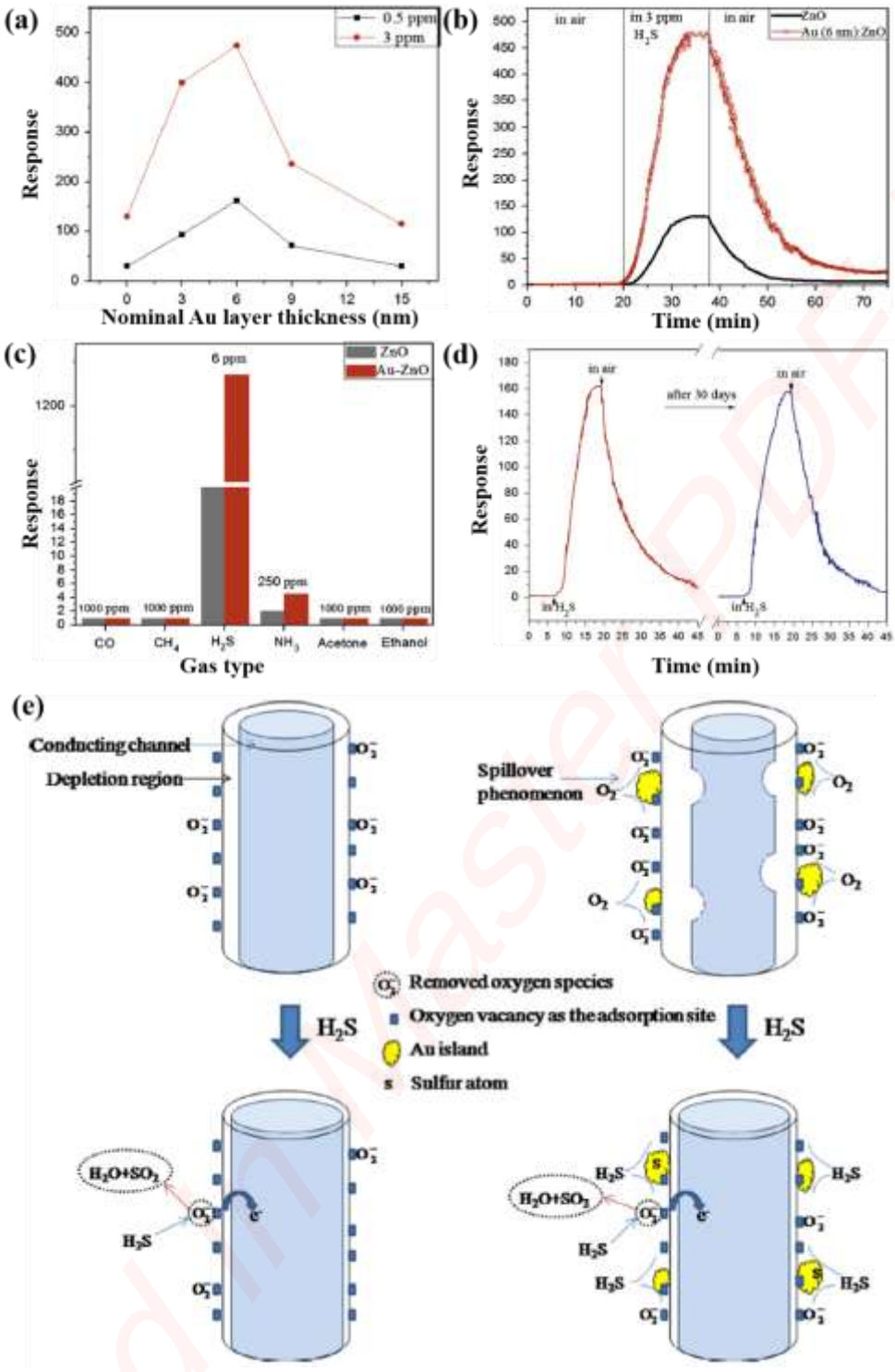

Fig. 10 (a) Variation of the sensor response of Au sensitized ZnO nanorods as a function of the Au nominal thickness toward 0.5 and 3 ppm H_2S at room temperature. (b) Dynamic response of pure and Au modified ZnO samples to 3 ppm H_2S. (c) Transient response of the Au (6 nm):ZnO sensor toward 0.5 ppm H_2S at room temperature after 30 days. (d) Response of the

pure and Au sensitized ZnO sensors to different gases at room temperature. (e) Schematic representation explaining the H_2S sensing mechanism [101].

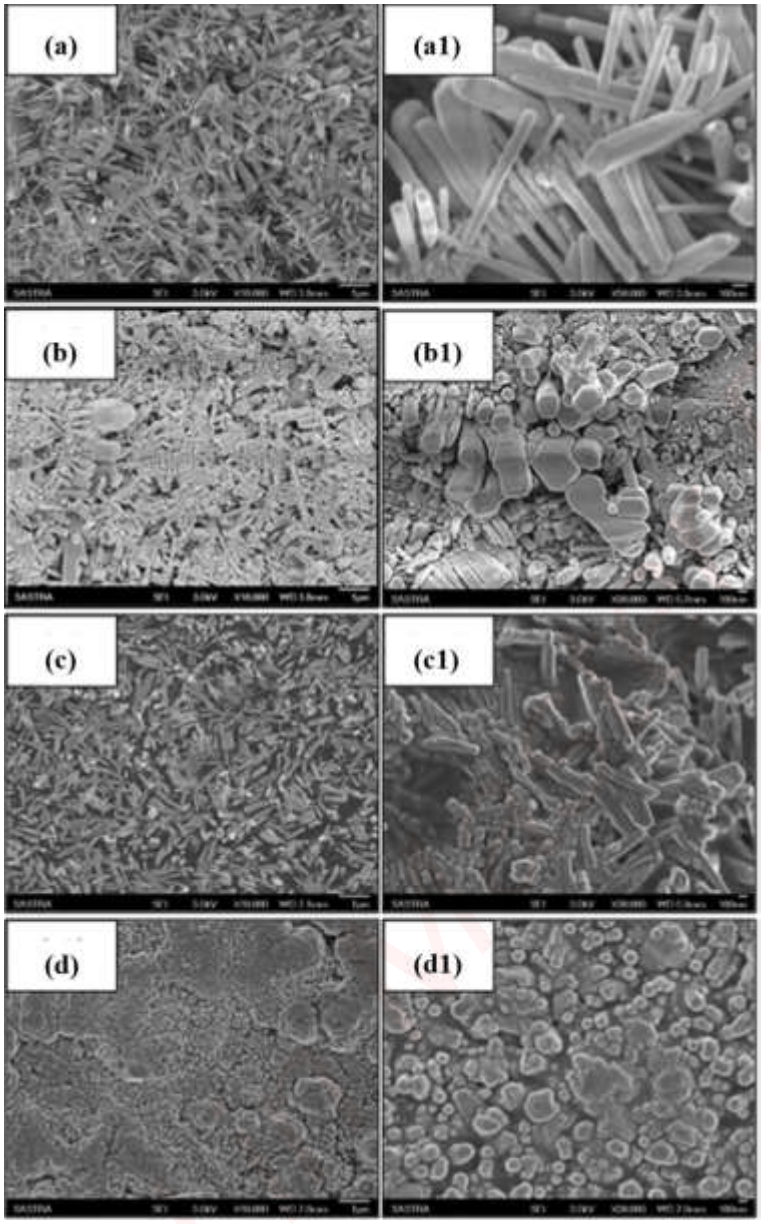

Fig. 11 FE-SEM images of (a) undoped, (b) Co-doped, (c) Ni-doped and (d) Cu-doped ZnO thin films. (a1)-(d1) shows the high magnification FE-SEM images respectively [98].

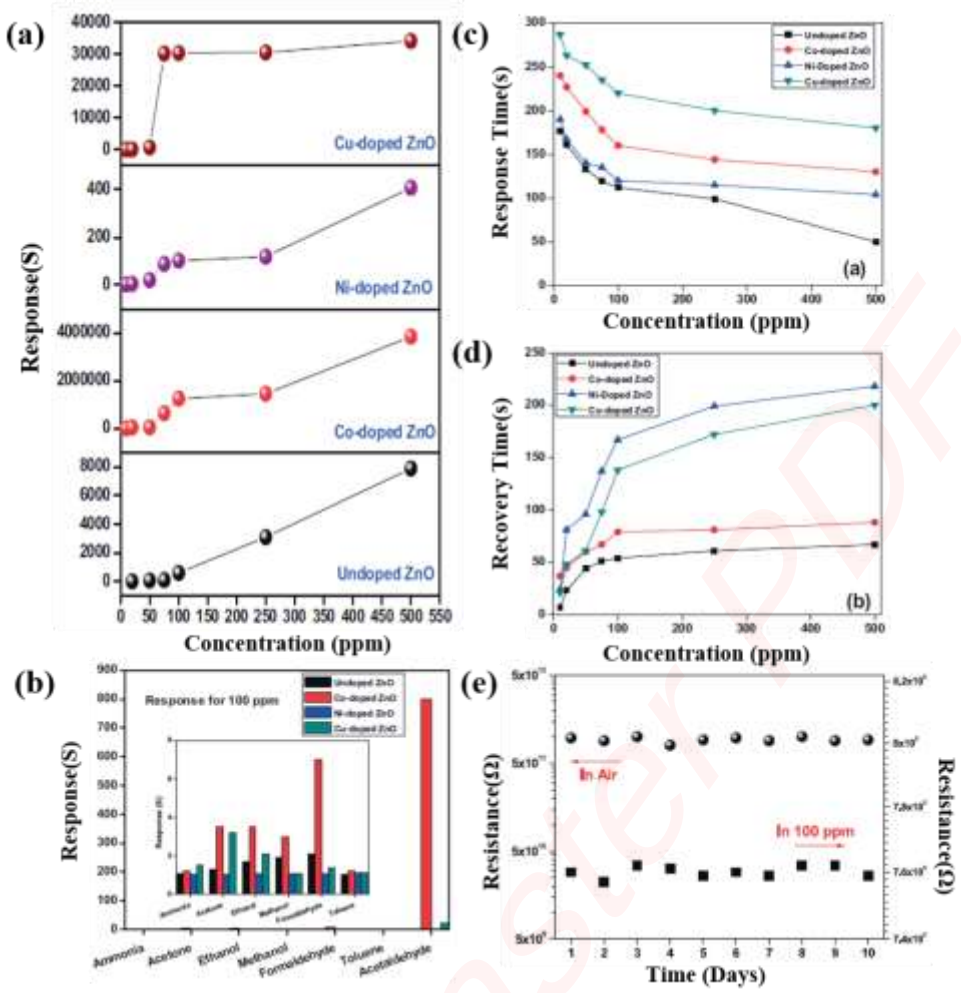

Fig. 12 (a) Response of undoped and doped ZnO thin films towards various concentrations of acetaldehyde at room temperature. (b) Selectivity nature of the sensing elements. Insert shows the highlighted view of response towards interfering vapors. (c) Response and (d) recovery times of undoped and doped ZnO nanostructures. (e) Stability nature of Co-doped ZnO thin films towards 100ppm over a period of 5 days [98].

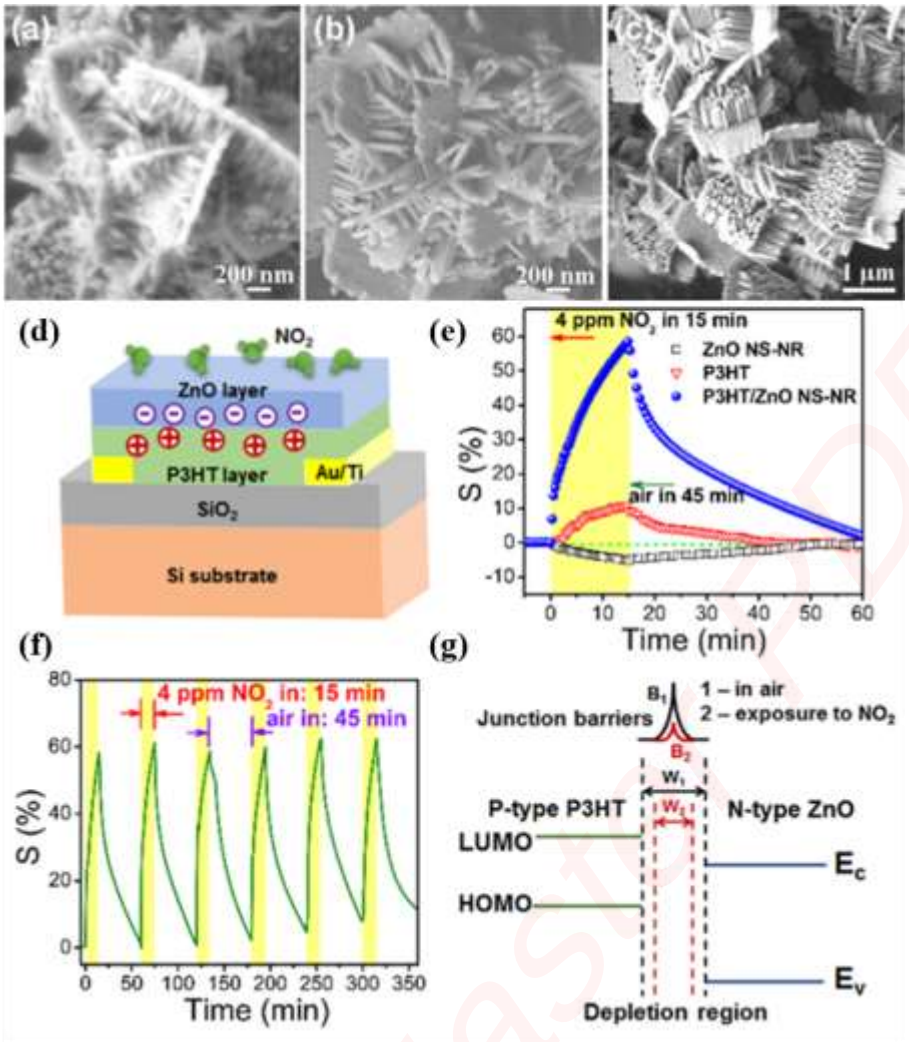

Fig. 13 SEM images of NS-NR in the products at $[OH^-]$ = 0.33 mol·L^{-1} with different aging time (min): (a) 20, (b) 30, (c) 40. (d) Schematic illustration for the gas sensor based on the P3HT/ZnO NS-NR bilayer hybrid film. (e) Dynamic response curves of the sensors based on pure ZnO NS-NR, pure P3HT film, and P3HT/ZnO NS-NR bilayer hybrid film to 4 ppm of NO_2 at room temperature. (f) Reproducibility of the hybrid sensors based on the P3HT/ZnO NS-NR composite films exposed to 4ppm of NO_2 at room temperature (for successive 6 cycles). (g) Energy-band of p-P3HT/n-ZnO heterojunction, showing the width of the depletion region and the junction barriers of the heterojunction in air and NO_2 [70].

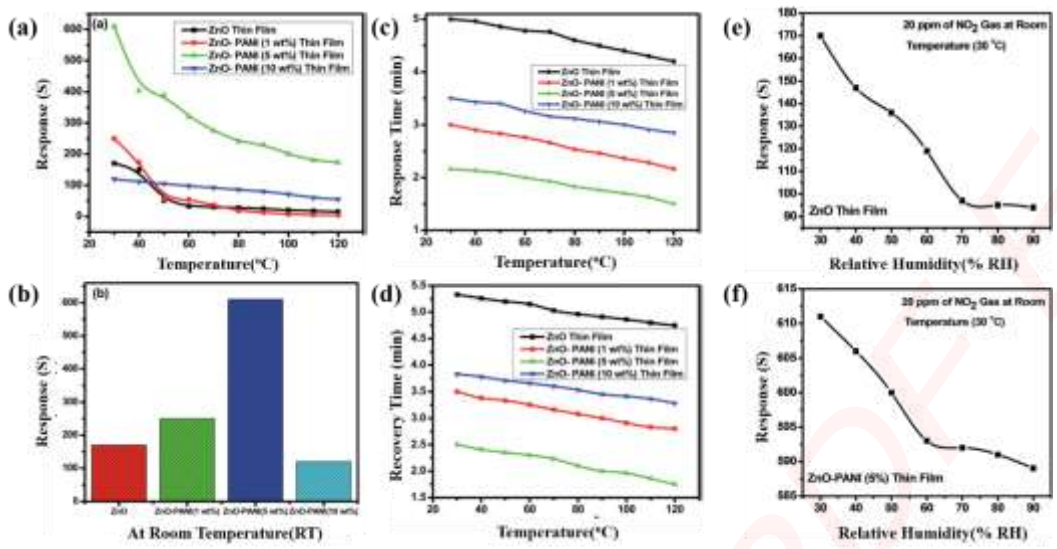

Fig. 14 Variation in sensing response (a) pure ZnO (b) ZnO-PANI (1 wt%), ZnO-PANI (5 wt%) and ZnO-PANI (10 wt%) thin film sensors as a function of temperature towards 20ppm of NO_2 gas. Variation in (c) response time and (d) recovery time of pure ZnO, ZnO-PANI (1 wt%), ZnO-PANI (5 wt%) and ZnO-PANI (10 wt%) thin film sensors. Variation of sensor response of (e) ZnO and (f) ZnO-PANI (5 wt%) with relative humidity (% RH) [105].

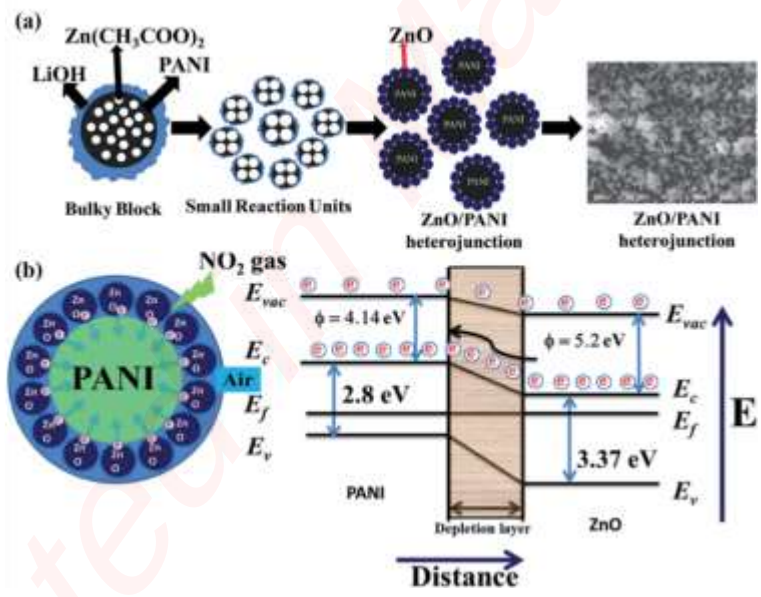

Fig. 15 (a) Schematic illustrating the mechanism of formation of ZnO/PANI heterojunction microstructure. (b) Schematic diagram of the proposed mechanism of NO_2 sensing of ZnO/PANI

heterojunctions [105].

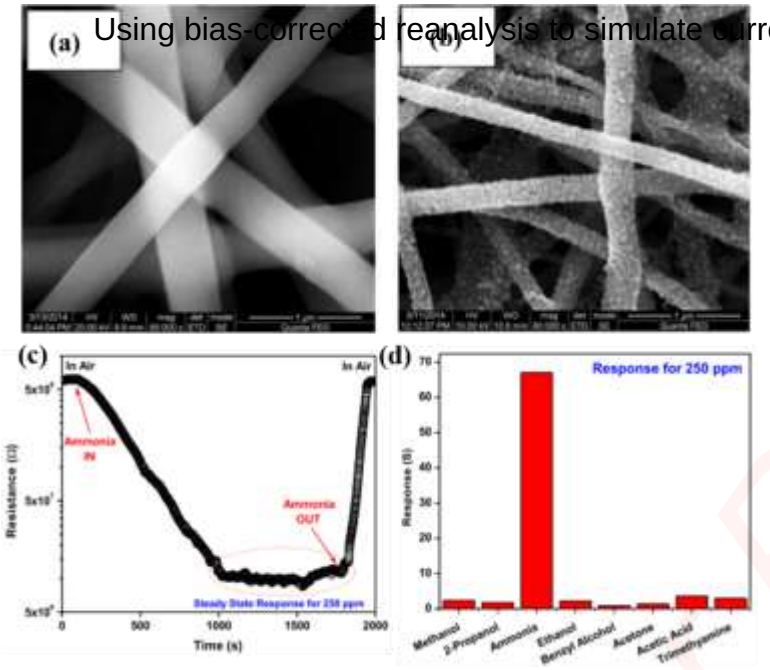

Fig. 16 SEM image of (a) as-spun and (b) annealed polyvinyl alcohol (PVA)-NiO-ZnO nanocomposite fibers. (c) Transient resistance response curve towards 250 ppm of ammonia. (d) Selectivity nature of the sensing element [114].

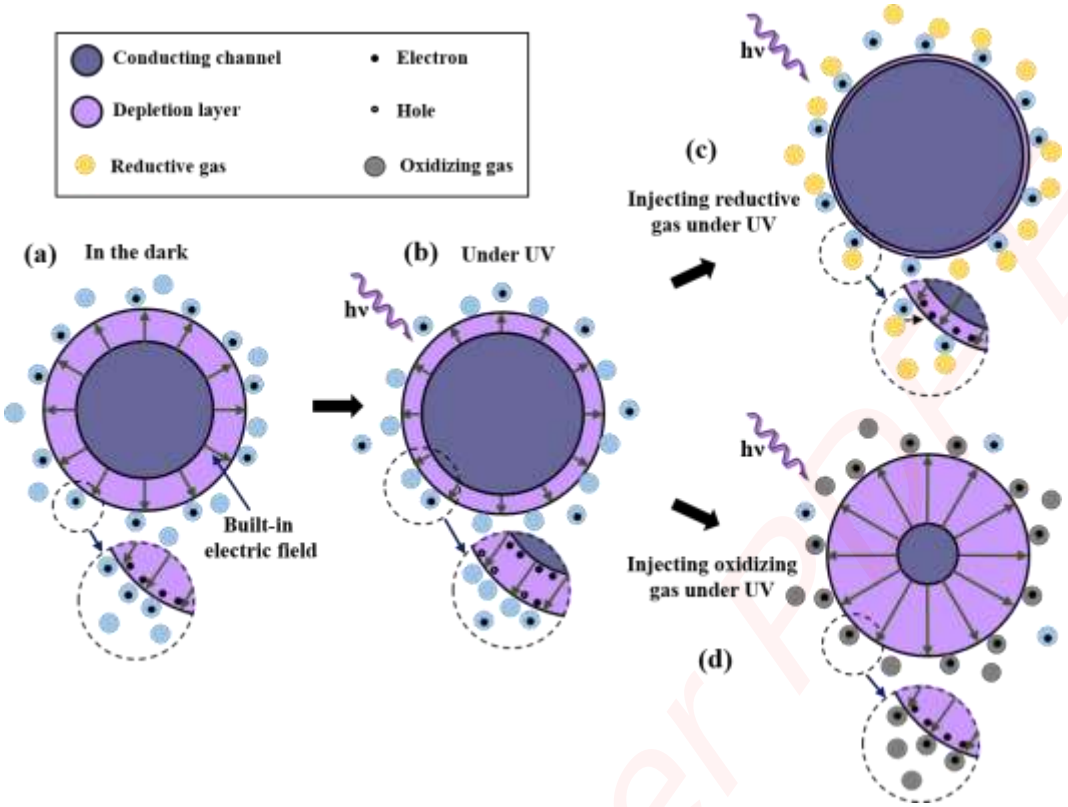

Fig. 17 Schematic of gas sensing process of ZnO under different working conditions: (a) in air, (b) in air under UV illumination, (c) in reductive test gas under UV illumination, (d) in oxidizing test gas under UV illumination.

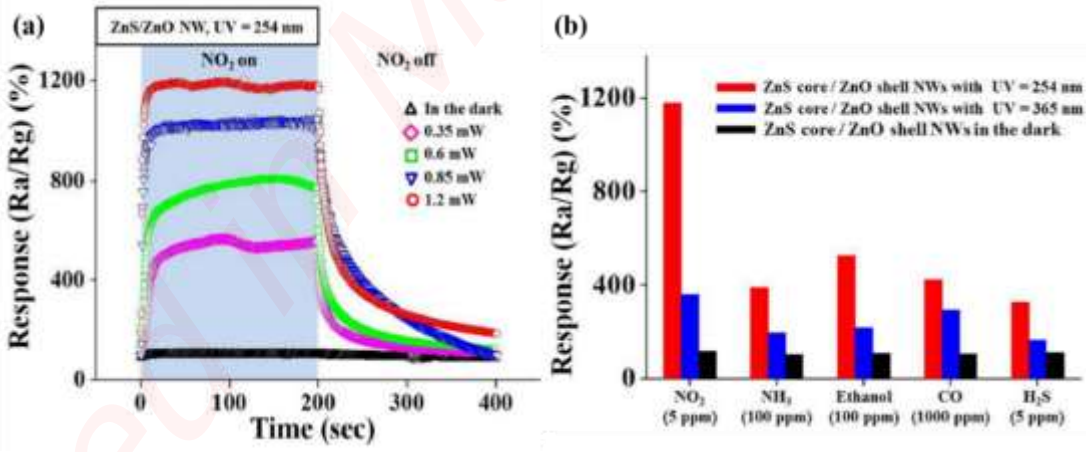

Fig. 18 (a) Dynamic responses of ZnS-core/ZnO-shell nanowires to 5 ppm NO_2 gas at room temperature under UV (254 nm) illumination at different illumination intensities. (b)

Comparison of responses of ZnS-core/ZnO-shell nanowires to different gases at room temperature in the dark and under UV (365 and 254 nm) illuminations [128].

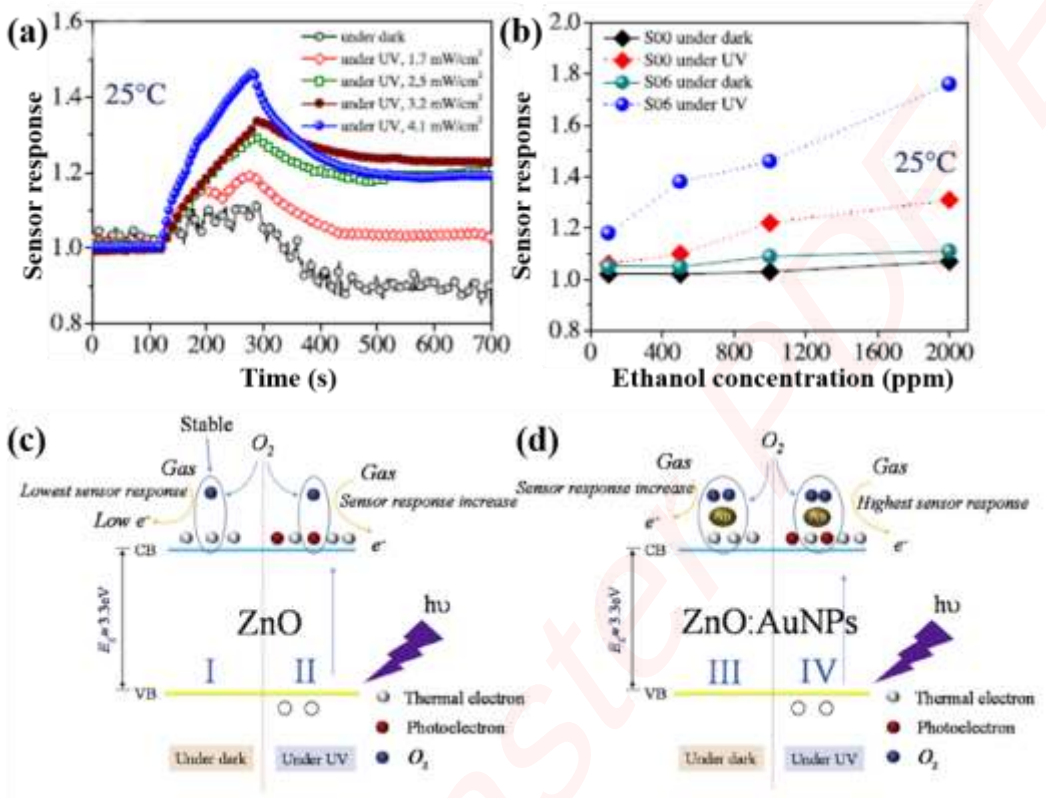

Fig. 19 (a) Dynamic sensor response of ZnO:AuNPs sensor at the sputtering time of 6 s (S06) upon exposure toward 1000ppm ethanol vapor with different UV illumination intensities operated at room temperature of 25ºC. (b) The linear ethanol response of the bare-ZnO (S00) and ZnO:AuNPs (S06) in the ethanol concentrations in the range of 100-2000 ppm under dark condition and UV illumination (4.1 mW/cm^2) at room temperature of 25ºC. Surface reaction mechanism of sensors based on (c) ZnO and (d) ZnO:AuNPs under dark condition and UV illumination [13].

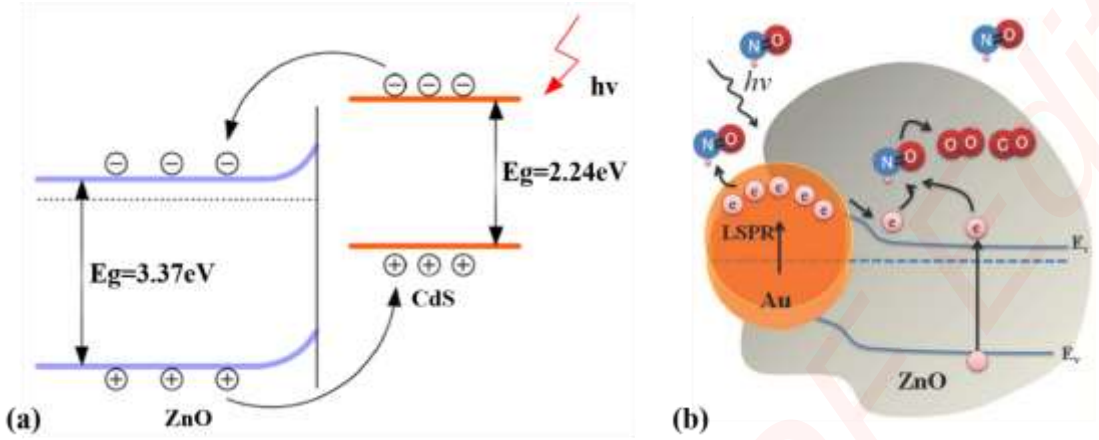

Fig. 20 (a) Schematic of the process of carriers formed in CdS-ZnO composite coating under visible light [23]. (b) Schematic illustration of NO gas sensing mechanism for Au-ZnO sensor under visible light illumination [131].

Table 1

A brief summary of sensor response of ZnO based gas sensors operating at relatively high temperature.

Material	Synthesis method	Target gas, concentration(ppm)	T_{opt}(°C)	Response	Ref.
Flower-like ZnO	Hydrothermal	Ethanol, 400	350	30.4	[25]
Cr-doped ZnO	Hydrothermal	Ethanol, 400	300	45	[52]
3-D hierarchical porous ZnO	Precipitation	Ethanol, 50	250	36.6	[53]
Al-doped ZnO	Modified sol-gel	CO, 80	250	~6	[54]
Co-doped ZnO	Hydrothermal	NO_2, 500	210	88	[55]
Ga-doped ZnO	Sol-gel	CO, 80	200	~5.5	[56]
CuO-decorated ZnO	Electrospinning	H_2S, 5	200	83.5	[57]
ZnO nanofibers	Electrospinning	Nitromethane, 30	170	29	[58]
W-doped ZnO	Magnetron sputtering	HCHO, 10	150	~350	[46]
ZnO thin film	Sol-gel	NH_3, 600	150	57.5%	[59]
ZnO nanoparticles	Hydrothermal	NH_3, 46	100	3.96%	[60]
ZnO QDs	Wet chemical	H_2S, 68.5	90	567	[61]

Note: T_{opt} = Operating temperature; QDs = Quantum dots.

Table 2

Comparison of the ZnO samples between the gas-sensing property and specific surface area [72].

Samples	HCHO concentration	Response	BET (m^2/g)
ZnO nanoplates	100 ppm	1.88	2.72
ZnO nanoflowers	100 ppm	4.95	4.68
ZnO nanofibers	100 ppm	12.61	9.61

Table 3

Room-temperature gas sensing performances of different morphological ZnO nanostructures.

Morphology	Synthesis method	Target gas, concentration(ppm)	Gas sensing performances			Ref.
			Response	Response time(s)	Recovery time(s)	
Nanorods	Carbothermal	Ethanol, 200	4.24	52	192	[74]
	Hydrothermal	H_2, 500	109%	149	122	[75]
	Microwave-assisted hydrothermal	NH_3, 20	~45%	33	51	[76]
	RF sputtering	NH_3, 25	~1%	64	28	[37]
	Two-step solution approach	H_2S, 1	11	500	360	[77]

	CVD	H_2S, 5	581	~1000	3700	[29]
	Spray pyrolysis	H_2S, 100	110	25	150	[78]
	Microwave-assisted chemical solution	H_2, 1000	294%	60	277	[79]
Nanowires	CVD	Ethanol, 20	~10%	NA	15	[42]
	CVD	H_2, 50 sccm	54%	NA	NA	[80]
	Carbothermal	Methanol, 0.5%	~8%	26	31	[81]
	Vacuum sucking	NH_3, 50	~65%	~28	~29	[82]
Nanoline	Soft e-beam lithography	H_2, 100	19%	NA	NA	[32]
		H_2, 200	~95%	NA	75	
Nanopetals	Chemical precipitation	NO_2, 20	~119	~85	103	[17]
Nanofibers	Electrospinning	HCHO, 100	12.61	NA	NA	[72]
Nanotubes	Electrodeposition, electrochemical etching	Ethanol, 10	30.91%	NA	NA	[71]
		Ethanol, 700	64.17	~274	~92	
Nanobelts	Carbothermal	H_2S, 10	8	NA	NA	[83]
Nanonails	Hydrothermal	H_2S, 100	70.4	35	82	[84]
Nanoflates	Hydrothermal	HCHO, 100	1.88	NA	NA	[72]
Nanoflatelets	Spray pyrolysis	Acetaldehyde, 50	50	60	40	[41]

Nanowalls	Solution route	NO_2, 5	~6.54	23	11	[18]
	RF sputtering	NH_3, 25	~1.5%	54	23	[85]
Nanocombs	CVD	CO, 500	8.93	400	55	[86]
Nanoflowers	Vapor phase transport	H_2S, 5	581	NA	NA	[29]
	Hydrothermal	HCHO, 100	4.95	NA	NA	[72]
Tapers	RF sputtering	NH_3, 25	~3%	49	19	[85]
Dendritic	vapor-phase transport	H_2S, 100	17.3	NA	NA	[87]
QDs	Colloidal progress	H_2S, 100	113.5	16	820	[88]
Thin film	Chemical	NO_2, 20	~119	~85	~103	[17]
	Sol-gel dip coating	NH_3, 100	1201.4	43	28	[89]
	Sol-gel dip coating	Acetone, 100	760	34	40	[90]
	Magnetron sputtering	NH_3, 100	~300	~92	113	[91]
	RF magnetron sputtering followed by SHI irradiation	NH_3, 600	~32	~20	~50	[73]
	Spray pyrolysis	NH_3, 25	233	20	25	[40]
	Spray pyrolysis	NH_3, 100	225	NA	NA	[39]

Spray pyrolysis	H_2, 450	81	NA	NA	[92]

Note: NA = Not available; QDs = Quantum dots.

Table 4

Room-temperature gas sensing performances of dopant/ZnO.

Dopant	Synthesis method	Target gas, concentration(ppm)	Gas sensing performances			Ref.
			Response	Response time(s)	Recovery time(s)	
Au	Microwave-assisted hydrothermal	NH_3, 100	1546.5	22	57	[93]
	Vapor phase transport, sputtering deposition	H_2S, 6	1270	NA	NA	[101]
	Hydrothermal, solution impregnation	CO, 50	~15	~8	~15	[116]
	Hydrothermal, RF Sputtering,	H_2S, 5	79.4	NA	NA	[95]
		H_2S, 1	38	NA	NA	[95]
	Sol-gel	HCHO, 5	10.57	138	104	[94]
Pt	RF magnetron sputtering	H_2, 0.1%	2.92	47	48	[97]
Cu	Microwave-assisted hydrothermal	NH_3, 100	~30%	13	33	[76]
	Spray pyrolysis	NH_3, 50	2667	30	12	[102]
Co	Spray pyrolysis	Acetaldehyde, 10	800	~240	~240	[98]
	Spray pyrolysis	NH_3, 100	3.48	36	10	[39]
Ni	Electrospinnig	HCHO, 100	532.7%	NA	NA	[14]
	Spray pyrolysis	H_2S, 100	321	12	90	[78]
Mg	Spray pyrolysis	NH_3, 100	796	34	28	[117]
	Spray pyrolysis	H_2, 100	~1.6	NA	NA	[118]
	RF sputtering	H_2, 200	~30	85	70	[119]
Sn	Sol-gel spin coating	N_2, 220 mL/min	2.53	NA	NA	[120]
La	Sol-gel	H_2, 1000	51%	NA	NA	[121]
P3HT	Spin coating	NO_2, 50	180%	NA	NA	[70]
PPy	In situ polymerization	NH_3, 1000	36.1%	2~5	600	[21]
PANI	Spin coating	NO_2, 20	661	129.6	210	[105]
PANI	Chemical oxidative process	Methanol, 100	1318	7	20	[122]

Porphyrin	Hydrothermal	CO, 10	~0.11	NA	NA	[123]
CuO	Plused laser deposition	H_2S, 0.5	~25%	~180	~15	[113]
NiO	Electrospinning	NH_3, 250	67	NA	NA	[114]
$CdSO_4$	Deposition	HCHO, 1	20%	NA	NA	[115]

Note: NA = Not available.

Table 5

Room-temperature gas sensing performances of ZnO based gas sensor under light irradiation.

Light source	Wavelength (nm)	Material	Synthesis method	Target gas, concentration(ppm)	Response	Ref.
UV	365	Ag/ZnO	Electrochemical Deposition	H_2,100	~50%	[125]
	365	ZnS/ZnO	Thermal evaporation, atom layer deposition	NO_2, 5	~350%	[128]
	365	Au/ZnO	CVD	H_2,5	21.5%	[135]
	365	Au/ZnO	Thermal evaporation, sputtering, thermal annealing	NO_2, 5	445%	[136]
	365	ZnO	Screen printing	HCHO, 100	1.5	[124]
	365	ZnO	Soft e-beam lithography	H_2, 100	19%	[32]
	365	Ni-doped ZnO	Electrospinning	HCHO, 100	532.7%	[14]
	365	Cr_2O_3/ZnO	Carbothermal, solvothermal	Ethanol, 200	1095%	[74]
	365	ZnO	Carbothermal	Ethanol, 200	424%	[74]
	365	SnO_2/ZnO	Thermal evaporation, atomic layer deposition	NO_2, 5	618.5%	[31]
	365	ZnO	Thermal evaporation, atomic layer deposition	NO_2, 5	103.8%	[31]
	351	ZnO	Hydrothermal	O_3, 0.1	~1.5	[129]
	254	ZnS/ZnO	Thermal evaporation, atom layer deposition	NO_2, 5	1180%	[128]

	254	Mn-doped ZnO	Spray pyrolysis	NO, 100	87%	[34]
	254	Au/ZnO	Thermal oxidation, sputtering	Ethanol, 100	1.18	[13]
Visible light	640	CdS/ZnO	Liquid plasma spray	NO_2, 1	15.3	[23]
	550	Au/ZnO	Photochemical	NO, 2	194%	[131]
	532	Au/ZnO	CVD, sputtering	C_2H_2, 100	~20%	[35]
	510	CdS/ZnO	Liquid plasma spray	NO_2, 1	31.9	[23]
	480	CdS/ZnO	Liquid plasma spray	NO_2, 1	25.1	[23]